

# Synthesis and Characterization of Osmium Nitrosyl Porphyrins Containing Organo, Halogeno, and $\mu$ -Oxo Ligands, and Extensions to the First Organometallic Thionitrosyl Porphyrin

Lin Cheng, Li Chen, Hee-Sun Chung, Masood A. Khan, and George B. Richter-Addo\*

Department of Chemistry and Biochemistry, University of Oklahoma, 620 Parrington Oval, Norman, Oklahoma 73019

Victor G. Young, Jr.

X-ray Structural Laboratory, Department of Chemistry, University of Minnesota, 207 Pleasant Street Southeast, Minneapolis, Minnesota 55455

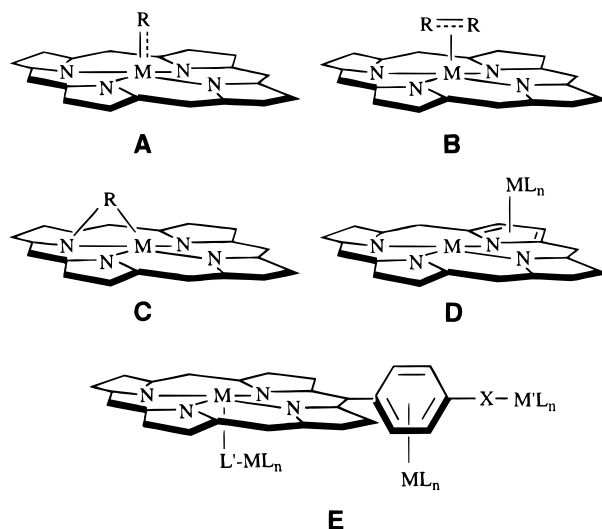
Received March 17, 1998

The sequential reaction of (OEP)Os(CO) with NOPF<sub>6</sub> (in CH<sub>2</sub>Cl<sub>2</sub>) followed by RMgX (in THF) gives variable isolated yields of the new (OEP)Os(NO)R (5–44%), (OEP)Os(R)<sub>2</sub> (1–10%), (OEP)Os(NO)X (14–19%), and [(OEP)Os(NO)]<sub>2</sub>( $\mu$ -O) (up to 24%) compounds, depending on the reaction conditions and the nature of R and X (OEP = octaethylporphyrinato dianion; R = Me, Et, <sup>t</sup>Pr, <sup>t</sup>Bu, *p*-C<sub>6</sub>H<sub>4</sub>F; X = Cl, Br). The IR  $\nu_{\text{NO}}$  values of the complexes (in CH<sub>2</sub>Cl<sub>2</sub>) decrease in the order (OEP)Os(NO)X (1799–1795 cm<sup>-1</sup>) > [(OEP)Os(NO)]<sub>2</sub>( $\mu$ -O) (1770 cm<sup>-1</sup>) > (OEP)Os(NO)R (1748–1703 cm<sup>-1</sup>). The  $\delta_{\text{meso}}$  peaks in the <sup>1</sup>H NMR spectra of the (OEP)-Os complexes (in CDCl<sub>3</sub>) also decrease in the order (OEP)Os(NO)X (10.41–10.40 ppm) > [(OEP)Os(NO)]<sub>2</sub>( $\mu$ -O) (10.35 ppm) > (OEP)Os(NO)R (10.24–10.21 ppm) > (OEP)Os(R)<sub>2</sub> (9.71–9.03 ppm). The thionitrosyl (OEP)Os(NS)Cl and (OEP)Os(NS)Me compounds have also been prepared. The solid-state molecular structures of [(OEP)Os(NO)]<sub>2</sub>( $\mu$ -O), (OEP)Os(NS)Cl, and (OEP)Os(NS)Me have been determined by single-crystal X-ray diffraction.

Several types of organometallic porphyrins are now known (Chart 1), and their varied natures have allowed diverse investigations into their chemical and spectroscopic properties.<sup>1–3</sup> Organometallic porphyrins of type **A** comprise those with metal–carbon(alkyl/aryl) single or multiple bonds. Dialkyl(aryl) complexes of the form (por)M(R)<sub>2</sub> have also been structurally characterized, and the  $\sigma$ -R ligands may either be located cis to each other (e.g., as in (OEP)Zr(Me)<sub>2</sub>)<sup>4,5</sup> or located trans to each other (e.g., as in (TTP)Os(CH<sub>2</sub>SiMe<sub>3</sub>)<sub>2</sub>) (OEP = 2,3,7,8,12,13,17,18-octaethylporphyrinato dianion, TTP = 5,10,15,20-tetra-*p*-tolylporphyrinato dianion).<sup>6,7</sup>

Organometallic porphyrins of type **B** include those with  $\eta^2$ -alkene/alkyne or other  $\pi$ -bonded groups such as cyclopentadienyl or indenyl ligands.<sup>1,9–12</sup> Type **C** complexes contain  $\mu$ -*N,M* units in which the bridging alkyl

Chart 1



(or carbene, vinyl, etc.) group maintains direct contact with the metal center.<sup>1,2,13,14</sup> The related nonorganometallic *N*-alkyl(aryl) porphyrins, in which there is no

(1) Brothers, P. J.; Collman, J. P. *Acc. Chem. Res.* **1986**, *19*, 209–215.

(2) Setsune, J.-I.; Dolphin, D. *Can. J. Chem.* **1987**, *65*, 459–467.

(3) Guillard, R.; Lecomte, C.; Kadish, K. M. *Struct. Bonding* **1987**, *64*, 205–268.

(4) Brand, H.; Arnold, J. *Organometallics* **1993**, *12*, 3655–3665.

(5) Brand, H.; Arnold, J. *Coord. Chem. Rev.* **1995**, *140*, 137–168.

(6) Leung, W.-H.; Hun, T. S. M.; Wong, K.-Y.; Wong, W.-T. *J. Chem. Soc., Dalton Trans.* **1994**, 2713–2718.

(7) A cis alkyl–hydroxyl complex has been recently proposed as an alternate intermediate in the cytochrome P450 rebound mechanism.<sup>8</sup>

(8) Collman, J. P.; Chien, A. S.; Eberspacher, T. A.; Brauman, J. I. *J. Am. Chem. Soc.* **1998**, *120*, 425–426.

(9) Collman, J. P.; Brothers, P. J.; McElwee-White, L.; Rose, E.; Wright, L. J. *J. Am. Chem. Soc.* **1985**, *107*, 4570–4571.

(10) Bartley, D. W.; Kodadek, T. *J. Am. Chem. Soc.* **1993**, *115*, 1656–1660.

(11) Collman, J. P.; Brothers, P. J.; McElwee-White, L.; Rose, E. *J. Am. Chem. Soc.* **1985**, *107*, 6110–6111.

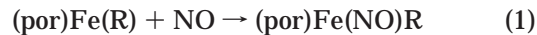
(12) Arnold, J.; Hoffman, C. G.; Dawson, D. Y.; Hollander, F. J. *Organometallics* **1993**, *12*, 3645–3654.

direct metal–alkyl(aryl) interaction, are also known.<sup>1,14–20</sup> Type **D** complexes have been reported recently, in which the pyrrole ring of a porphyrin fragment is  $\pi$ -bound to a second metal moiety.<sup>21–23</sup> Type **E** complexes have been described, in which an external metal-containing fragment is (i) bound to an aryl substituent in either a  $\pi$ - or  $\sigma$ -bound fashion or (ii) bound via an organic moiety to the central metal of the metalloporphyrin.<sup>26–29</sup>

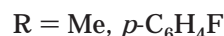
Interest in the study of organometallic complexes containing a direct M–R interaction (e.g., in types **A–C**) results from the detection and/or postulation of organometallic species in the natural and model chemistry of coenzyme B<sub>12</sub>, cytochrome P450, and other heme-containing biomolecules.<sup>1,2,30,31</sup> In this regard, many Co model systems for coenzyme B<sub>12</sub> have been synthesized and studied.<sup>32–36</sup>

The reported organometallic chemistry of group 8 metalloporphyrins has so far been focused on those of iron<sup>3,37–40</sup> and ruthenium.<sup>9,11,14,15,18,41–49</sup> Surprisingly,

only a handful of organoosmium porphyrins have been reported to date.<sup>6,11,43,49,50</sup> Interestingly, some (por)Fe(R) complexes (of type **A**) react with NO gas to form nitrosyl adducts (eq 1).<sup>51,52</sup> In some cases, the known



(por)Fe(NO) complexes are produced instead. We recently reported the synthesis and characterization of analogous Ru complexes (type **A**) via the reaction of the (TTP)Ru(NO)Cl precursor with Grignard reagents (eq 2).<sup>44</sup> We also reported the single-crystal X-ray struc-



tural characterization of a representative complex, namely that of (TTP)Ru(NO)(*p*-C<sub>6</sub>H<sub>4</sub>F). We attempted to extend the reaction outlined in eq 2 to osmium porphyrins but were only able to obtain the desired organoosmium products in very low (<5%) yields. However, we have found that the sequential reaction of (por)Os(CO) with NOPF<sub>6</sub> and then RMgX gives isolable quantities of the desired (por)Os(NO)R complexes (type **A**) together with other Os nitrosyl and non-nitrosyl porphyrin products. This latter finding is the subject of this paper. To the best of our knowledge, this is the first report on organoosmium nitrosyl porphyrins. Our successful extension to the synthesis and structural characterization of osmium thionitrosyl porphyrins is also reported.

## Experimental Section

**General Comments.** All reactions were performed under an atmosphere of prepurified nitrogen using standard Schlenk techniques and/or in an Innovative Technology Labmaster 100 Dry Box unless stated otherwise. All column chromatography was done under nitrogen. Solvents were distilled from appropriate drying agents under nitrogen just prior to use: CH<sub>2</sub>-Cl<sub>2</sub> (CaH<sub>2</sub>), THF (Na/benzophenone), hexane (Na/benzophenone/tetraglyme), and benzene (Na). Solutions for spectral studies were prepared under a nitrogen atmosphere and measured immediately.

**Chemicals.** (TTP)Os(CO) and (OEP)Os(CO) were prepared by literature methods (TTP = 5,10,15,20-tetra-*p*-tolylporphyrinato dianion, OEP = 2,3,7,8,12,13,17,18-octaethylporphyrinato dianion).<sup>54</sup> (NSCl)<sub>3</sub> was prepared by literature method.<sup>55</sup> The labeled (<sup>15</sup>NSCl)<sub>3</sub> analogue was prepared similarly using <sup>15</sup>NH<sub>4</sub>Cl (Isotec). Nitrosyl chloride was prepared by the

(13) Setsune, J.-I.; Saito, Y.; Ishimaru, Y.; Ikeda, M.; Kitao, T. *Bull. Chem. Soc. Jpn.* **1992**, *65*, 639–648.

(14) Seyler, J. W.; Safford, L. K.; Fanwick, P. E.; Leidner, C. R. *Inorg. Chem.* **1992**, *31*, 1545–1547.

(15) Seyler, J. W.; Leidner, C. R. *Inorg. Chem.* **1990**, *29*, 3636–3641.

(16) Lançon, D.; Cocolios, P.; Guillard, R.; Kadish, K. M. *J. Am. Chem. Soc.* **1984**, *106*, 4472–4478.

(17) Guillard, R.; Boisselier-Cocolios, B.; Tabard, A.; Cocolios, P.; Simonet, B.; Kadish, K. M. *Inorg. Chem.* **1985**, *24*, 2509–2520.

(18) Seyler, J. W.; Leidner, C. R. *J. Chem. Soc., Chem. Commun.* **1989**, 1794–1796.

(19) Dolphin, D.; Halko, D. J.; Johnson, E. *Inorg. Chem.* **1981**, *20*, 4348–4351.

(20) Bartczak, T. J.; Latos-Grazynski, L.; Wyslouch, A. *Inorg. Chim. Acta* **1990**, *171*, 205–212.

(21) Senge, M. O. *Angew. Chem., Int. Ed. Engl.* **1996**, *35*, 1923–1925 and references therein.

(22) Dailey, K.; Rauchfuss, T. B. *Polyhedron* **1997**, *16*, 3129–3136.

(23) Related  $\eta^5$ -pyrrole porphyrinogen complexes have also been structurally characterized.<sup>24,25</sup>

(24) Jacoby, D.; Isoz, S.; Floriani, C.; Chiesi-Villa, A.; Rizzoli, C. *J. Am. Chem. Soc.* **1995**, *117*, 2805–2816.

(25) Jacoby, D.; Isoz, S.; Floriani, C.; Chiesi-Villa, A.; Rizzoli, C. *J. Am. Chem. Soc.* **1995**, *117*, 2793–2804.

(26) Uosaki, K.; Kondo, T.; Zhang, X.-Q.; Yanagida, M. *J. Am. Chem. Soc.* **1997**, *119*, 8367–8368.

(27) Beer, P. D.; Drew, M. G. B.; Jagessar, R. *J. Chem. Soc., Dalton Trans.* **1997**, 881–886.

(28) Wagner, R. W.; Brown, P. A.; Johnson, T. E.; Lindsey, J. S. *J. Chem. Soc., Chem. Commun.* **1991**, 1463–1466.

(29) Zakrzewski, J.; Giannotti, C. *Coord. Chem. Rev.* **1995**, *140*, 169–187.

(30) Mansuy, D. *Pure Appl. Chem.* **1987**, *59*, 759–770.

(31) Krättiler, B. In *Encyclopedia of Inorganic Chemistry*; King, R. B., Ed.; John Wiley and Sons: Chichester, 1994; Vol. 2, pp 697–712.

(32) Brown, K.; Cheng, S.; Zou, X.; Zubkowski, J. D.; Valente, E. J.; Knapton, L.; Marques, H. M. *Inorg. Chem.* **1997**, *36*, 3666–3675.

(33) Gridnev, A. A.; Ittel, S. D.; Fryd, M.; Wayland, B. B. *Organometallics* **1996**, *15*, 222–235.

(34) Summers, J. S.; Petersen, J. L.; Stolzenberg, A. M. *J. Am. Chem. Soc.* **1994**, *116*, 7189–7195.

(35) Kadish, K. M.; Han, B. C.; Endo, A. *Inorg. Chem.* **1991**, *30*, 4502–4506.

(36) Chopra, M.; Hun, T. S. M.; Leung, W.-H.; Yu, N.-T. *Inorg. Chem.* **1995**, *34*, 5973–5978.

(37) Arafa, I. M.; Shin, K.; Goff, H. M. *J. Am. Chem. Soc.* **1988**, *110*, 5228–5229.

(38) Li, Z.; Goff, H. M. *Inorg. Chem.* **1992**, *31*, 1547–1548.

(39) Song, B.; Goff, H. M. *Inorg. Chim. Acta* **1994**, *226*, 231–235.

(40) Kadish, K. M.; Tabard, A.; Lee, W.; Liu, Y. H.; Ratti, C.; Guillard, R. *Inorg. Chem.* **1991**, *30*, 1542–1549.

(41) Alexander, C. S.; Rettig, S. J.; James, B. R. *Organometallics* **1994**, *13*, 2542–2544.

(42) Collman, J. P.; McElwee-White, L.; Brothers, P. J.; Rose, E. *J. Am. Chem. Soc.* **1986**, *108*, 1332–1334.

(43) Collman, J. P.; Rose, E.; Venburg, G. D. *J. Chem. Soc., Chem. Commun.* **1994**, 11–12.

(44) Hodge, S. J.; Wang, L.-S.; Khan, M. A.; Young, V. G.; Richter-Addo, G. B. *Chem. Commun.* **1996**, 2283–2284.

(45) Ke, M.; Rettig, S. J.; James, B. R.; Dolphin, D. *J. Chem. Soc., Chem. Commun.* **1987**, 1110–1112.

(46) Sishta, C.; Ke, M.; James, B. R.; Dolphin, D. *J. Chem. Soc., Chem. Commun.* **1986**, 787–788.

(47) Ke, M.; Sishta, C.; James, B. R.; Dolphin, D.; Sparapany, J. W.; Ibers, J. A. *Inorg. Chem.* **1991**, *30*, 4766–4771.

(48) Seyler, J. W.; Fanwick, P. E.; Leidner, C. R. *Inorg. Chem.* **1992**, *31*, 3699–3700.

(49) Collman, J. P.; Ha, Y.; Wagenknecht, P. S.; Lopez, M.-A.; Guillard, R. *J. Am. Chem. Soc.* **1993**, *115*, 9080–9088.

(50) The organometallic chemistry of Ru and Os complexes with  $\eta^1$ -carbon ligands has been reviewed, see: Hill, A. F. In *Comprehensive Organometallic Chemistry II. A Review of the Literature 1982–1994*, 1st ed.; Abel, E. W., Stone, F. G. A., Wilkinson, G., Eds.; Pergamon: Exeter, U.K., 1995; Vol. 7, pp 299–440.

(51) Guillard, R.; Lagrange, G.; Tabard, A.; Lançon, D.; Kadish, K. M. *Inorg. Chem.* **1985**, *24*, 3649–3656.

(52) The (TPP)Fe(NO)(C<sub>5</sub>H<sub>5</sub>) complex has been claimed to be isolated,<sup>53</sup> although its reported  $\nu_{\text{NO}}$  of 1705 cm<sup>-1</sup> is very close to that of the known (TPP)Fe(NO) ( $\nu_{\text{NO}}$  = 1699 cm<sup>-1</sup>).

literature method.<sup>56</sup> NOPF<sub>6</sub> (96%) and all Grignard reagents used were purchased from Aldrich Chemical Co. Chloroform-*d* (99.8%) and benzene-*d*<sub>6</sub> (99.6%) were obtained from Cambridge Isotope Laboratories, subjected to 3 freeze-pump-thaw cycles, and stored over Linde 4 Å molecular sieves. Elemental analyses were performed by Atlantic Microlab, Norcross, GA.

**Instrumentation.** Infrared spectra were recorded on a Bio-Rad FT-155 FTIR spectrometer. <sup>1</sup>H NMR spectra were obtained on a Varian 400 MHz spectrometer, and the signals (in ppm) were referenced to the residual signal of the solvent employed. All couplings are in hertz. FAB mass spectra were obtained on a VG-ZAB-E mass spectrometer. UV-vis spectra were recorded on a Hewlett-Packard model 8453 diode array instrument. Wavelengths are reported with  $\epsilon$  values or as %-intensities for the samples whose yields were too small for accurate concentration measurements.

**Preparation of (Porphyrin)Os(NO)(R) Compounds (R = 'Bu, 'Pr, Et, Me, *p*-C<sub>6</sub>H<sub>4</sub>F).** These compounds were synthesized either at low temperature or at room temperature.

**Method I.** The following reaction is representative: To a solution of (OEP)Os(CO) (0.080 g, 0.107 mmol) in CH<sub>2</sub>Cl<sub>2</sub> (10 mL) was added NOPF<sub>6</sub> (0.020 g, 0.114 mmol). The mixture was stirred under reduced lighting for 1 h. The solvent was removed in vacuo, and the resulting dark red solid was redissolved in THF (10 mL). The mixture was cooled to -30 °C, and 'BuMgCl (0.30 mL, 0.30 mmol, 1.0 M in THF) was added dropwise. The stirred reaction mixture was kept between -20 and -30 °C. Monitoring the reaction by TLC (silica gel, 1:1 benzene/hexane) showed that the [(OEP)Os(NO)]-PF<sub>6</sub> intermediate was consumed within a 30 min period. The solvent was removed in vacuo. The red residue was dissolved in a minimum amount of benzene and chromatographed (under nitrogen) on an alumina column (2 × 40 cm) prepared in hexane. Eluting with a benzene/hexane (1:1) mixture yielded a brown band and a red band, which were collected separately. Removal of solvent from the brown fraction gave (OEP)Os('Bu)<sub>2</sub> (0.002 g, 2% yield). Removal of solvent from the red fraction gave (OEP)Os(NO>('Bu) as a red solid (0.021 g, 24% yield). Elution was next performed with a CH<sub>2</sub>Cl<sub>2</sub>/hexane (1:1) mixture, and a second red band was collected. Solvent removal from this fraction gave red crystals of (OEP)Os(NO)Cl (0.003 g, 4% yield). Finally, a fourth red band was eluted with a THF/hexane (1:1) solvent mixture. Removal of the solvent from this fraction gave a residue that was recrystallized from a CH<sub>2</sub>Cl<sub>2</sub>/hexane mixture in air to give the [(OEP)Os(NO)]<sub>2</sub>( $\mu$ -O) oxo dimer (0.010 g, 0.007 mmol, 12% yield based on Os).

The (OEP)Os(NO)(Pr) compound was generated similarly (using 'PrMgCl, 2.0 M in Et<sub>2</sub>O, 3-fold excess, 30 min reaction time) in 25% yield, with (OEP)Os('Pr)<sub>2</sub> (1%), (OEP)Os(NO)Cl (4%), and [(OEP)Os(NO)]<sub>2</sub>( $\mu$ -O) (8%) as the other isolated products.

The (OEP)Os(NO)(Et) compound was generated similarly (using EtMgCl, 1.0 M in THF, 3-fold excess, 25 min reaction time) in 17% yield, with (OEP)Os(Et)<sub>2</sub> (5%), (OEP)Os(NO)Cl (6%), and [(OEP)Os(NO)]<sub>2</sub>( $\mu$ -O) (8%) as the other isolated products.

The (OEP)Os(NO)(Me) compound was generated similarly in ca. 5% yield using (i) MeMgBr (1.4 M in toluene/THF, 2-fold excess, 1.5 h reaction time) with (OEP)Os(NO)Br (17%) and [(OEP)Os(NO)]<sub>2</sub>( $\mu$ -O) (12%) as the other isolated products or (ii) MeMgCl (3.0 M in THF, 15-fold excess, 1.5 h reaction time) with (OEP)Os(NO)Cl (16%) and [(OEP)Os(NO)]<sub>2</sub>( $\mu$ -O) (24%) as the other isolated products.

The (OEP)Os(NO)(*p*-C<sub>6</sub>H<sub>4</sub>F) compound was generated similarly using (*p*-C<sub>6</sub>H<sub>4</sub>F)MgBr (1.0 M in THF, 6-fold excess, 30 min reaction time) in 13% yield, with (OEP)Os(*p*-C<sub>6</sub>H<sub>4</sub>F)<sub>2</sub> (3%), (OEP)Os(NO)Br (19%), and [(OEP)Os(NO)]<sub>2</sub>( $\mu$ -O) (<5%) as the other isolated products. When the reaction was performed at room temperature (see next section), however, only (OEP)Os(NO)(*p*-C<sub>6</sub>H<sub>4</sub>F) and (OEP)Os(*p*-C<sub>6</sub>H<sub>4</sub>F)<sub>2</sub> were formed in 20% and 10% isolated yields, respectively (i.e., the intermediate (OEP)Os(NO)Br is consumed in the reaction).

**Method II.** The following reaction is representative of the room-temperature reactions: To a CH<sub>2</sub>Cl<sub>2</sub> (20 mL) solution of (OEP)Os(CO) (0.060 g, 0.08 mmol) was added NOPF<sub>6</sub> (96%, 0.015 g, 0.082 mmol). The color of the solution changed from pink to dark red. The mixture was left to stir for 30 min, and all the solvent was removed. The solid was redissolved in THF (20 mL) at room temperature, and excess MeMgBr (0.7 mmol) was added. No substantial color change was observed. The solvent was removed immediately after adding the MeMgBr reagent, and the residue was dissolved in a minimum amount of benzene and quickly filtered through a silica gel column. All the solvent was removed from the filtrate, and the red solid was dried in vacuo for 5 h to give (OEP)Os(NO)(Me) (0.027 g, 0.035 mmol, 44% yield).

The (OEP)Os(NO)(Pr) compound was prepared similarly in 30% yield.

The (TTP)Os(NO)Me compound was generated similarly in 35% yield from the sequential reaction of (TTP)Os(CO) with NOPF<sub>6</sub> and then MeMgCl as described above.

A 2:1 mixture of (OEP)Os(NO)Et and (OEP)Os(Et)<sub>2</sub> is produced from the room-temperature reaction (using EtMgCl) in 39% overall yield.

**Alternate Preparation of (OEP)Os(NO)Cl and [(OEP)Os(NO)]<sub>2</sub>( $\mu$ -O).** To a CH<sub>2</sub>Cl<sub>2</sub> (20 mL) solution of (OEP)Os(CO) (0.060 g, 0.080 mmol) was added ClNO (0.081 mmol in CH<sub>2</sub>Cl<sub>2</sub>) dropwise at room temperature. The reaction mixture was stirred for 15 min. The color of the solution turned from pink red to bright red. The reaction mixture was transferred to the top of an alumina column and filtered using CH<sub>2</sub>Cl<sub>2</sub> as eluent. This filtrate was collected and taken to dryness, and the red residue was dried in vacuo for 2 h to give (OEP)Os(NO)Cl (0.031 g, 0.039 mmol, 49% yield). The alumina column was then washed with THF, and a resulting second filtrate was obtained and collected. The solvent was removed, and the red residue was recrystallized from CH<sub>2</sub>Cl<sub>2</sub> (by slow solvent evaporation under nitrogen) to give [(OEP)Os(NO)]<sub>2</sub>( $\mu$ -O) (0.029 g, 0.019 mmol, 48% yield based on Os).

**(OEP)Os(NO)(Bu).** Anal. Calcd for C<sub>40</sub>H<sub>53</sub>N<sub>5</sub>OOS: C, 59.31; H, 6.59; N, 8.65. Found: C, 59.91; H, 6.73; N, 8.38. IR (CH<sub>2</sub>Cl<sub>2</sub>, cm<sup>-1</sup>):  $\nu_{\text{NO}}$  1703. IR (KBr, cm<sup>-1</sup>):  $\nu_{\text{NO}}$  1716 s; also 2964 m, 2931 w, 2867 w, 2832 w, 1465 m, 1445 m, 1372 w, 1316 w, 1272 m, 1228 w, 1153 m, 1110 w, 1056 m, 1020 m, 994 w, 962 w, 840 w, 746 w. <sup>1</sup>H NMR (CDCl<sub>3</sub>,  $\delta$ ): 10.23 (s, 4H, *meso*-H of OEP), 4.12 (q, *J* = 8, 16H, CH<sub>2</sub>CH<sub>3</sub> of OEP), 1.95 (t, *J* = 8, 24H, CH<sub>2</sub>CH<sub>3</sub> of OEP), -4.66 (s, 9H, 'Bu). Low-resolution mass spectrum (FAB): *m/z* 754 [(OEP)Os(NO)]<sup>+</sup> (57). UV-vis spectrum ( $\lambda$ , benzene): 366 (100, Soret), 446 (45), 554 (18), 579 (br sh, 13) nm.

**(OEP)Os(NO)(Pr).** Anal. Calcd for C<sub>39</sub>H<sub>51</sub>N<sub>5</sub>OOS·0.35CH<sub>2</sub>Cl<sub>2</sub>: C, 57.23; H, 6.31; N, 8.48; Cl, 3.01. Found: C, 57.34; H, 6.57; N, 7.73; Cl, 2.83. IR (CH<sub>2</sub>Cl<sub>2</sub>, cm<sup>-1</sup>):  $\nu_{\text{NO}}$  1703. IR (KBr, cm<sup>-1</sup>):  $\nu_{\text{NO}}$  1715 s; also 2965 w, 2928 w, 2868 w, 1609 m, 1534 vw, 1464 m, 1446 m, 1372 m, 1316 w, 1272 m, 1218 w, 1151 m, 1110 w, 1056 m, 1019 s, 994 m, 962 m, 839 w, 803 w, 744 m, 713 w. <sup>1</sup>H NMR (CDCl<sub>3</sub>,  $\delta$ ): 10.21 (s, 4H, *meso*-H of OEP), 5.28 (s, CH<sub>2</sub>Cl<sub>2</sub>), 4.12 (q, *J* = 8, 16H, CH<sub>3</sub>CH<sub>2</sub> of OEP), 1.96 (t, *J* = 8, 24H, CH<sub>3</sub>CH<sub>2</sub> of OEP), -4.63 (d, *J* = 7, 6H, (CH<sub>3</sub>)<sub>2</sub>CH of 'Pr), -7.12 (sept, *J* = 7, 1H, (CH<sub>3</sub>)<sub>2</sub>CH of 'Pr). Low-resolution mass spectrum (FAB): *m/z* 798 [(OEP)Os(NO)(Pr) + H]<sup>+</sup> (6), 767 [(OEP)Os('Pr)]<sup>+</sup> (9), 754 [(OEP)Os(NO)]<sup>+</sup> (27), 724 [(OEP)Os]<sup>+</sup> (15). UV-vis spectrum ( $\lambda$ ,  $\epsilon$ , mM<sup>-1</sup> cm<sup>-1</sup>): 1.68 × 10<sup>-5</sup> M in CH<sub>2</sub>Cl<sub>2</sub>: 359 (62), 446 (34), 552 (13), 582 (8) nm.

(53) Massoudipour, M.; Tewari, S. K.; Pandey, K. K. *Polyhedron* **1989**, *8*, 1447-1451.

(54) Che, C.-M.; Poon, C.-K.; Chung, W.-C.; Gray, H. B. *Inorg. Chem.* **1985**, *24*, 1277-1278.

(55) Jolly, W. L.; Maguire, K. D. *Inorg. Synth.* **1967**, *9*, 102-111.

(56) Pass, G.; Sutcliffe, H. *Practical Inorganic Chemistry: Preparations, Reactions and Instrumental Methods*; Chapman and Hall: London, U.K., 1968; pp 145-146.

**(OEP)Os(NO)Et.** Anal. Calcd for  $C_{38}H_{49}N_5O_2$ : C, 58.36; H, 6.32; N, 8.96. Found: C, 58.12; H, 6.29; N, 8.70. IR ( $CH_2Cl_2$ ,  $cm^{-1}$ ):  $\nu_{NO}$  1710. IR (KBr,  $cm^{-1}$ ):  $\nu_{NO}$  1717 s; also 2967 m, 2933 w, 2871 w, 1272 w, 1152 w, 1111 w, 1056 w, 1020 m, 995 w, 964 w, 839 w, 745 w.  $^1H$  NMR ( $CDCl_3$ ,  $\delta$ ): 10.21 (s, 4H, *meso*-H of OEP), 4.12 (q,  $J = 8$ , 16H,  $CH_2CH_3$  of OEP), 1.96 (t,  $J = 8$ , 24H,  $CH_2CH_3$  of OEP), -4.62 (t,  $J = 8$ , 3H,  $CH_3$  of Et), -7.45 (q,  $J = 8$ , 2H,  $CH_2$  of Et). UV-vis spectrum ( $\lambda$ ,  $CH_2Cl_2$ ): 355 (100, Soret), 446 (61), 553 (22), 583 (12) nm.

**(OEP)Os(NO)Me.** IR ( $CH_2Cl_2$ ,  $cm^{-1}$ ):  $\nu_{NO}$  1720. IR (KBr,  $cm^{-1}$ ):  $\nu_{NO}$  1732 s; also 2966 w, 2932 w, 2869 w, 1467 m, 1446 m, 1372 w, 1317 w, 1272 m, 1227 w, 1151 m, 1111 w, 1056 m, 1020 s, 994 m, 964 m, 838 m, 802 w, 745 m, 713 m, 518 w.  $^1H$  NMR ( $CDCl_3$ ,  $\delta$ ): 10.21 (s, 4H, *meso*-H of OEP), 4.12 (q,  $J = 8$ , 16H,  $CH_2CH_3$  of OEP), 1.97 (t,  $J = 8$ , 24H,  $CH_2CH_3$  of OEP), -8.10 (s, 3H,  $CH_3$ ). Low-resolution mass spectrum (FAB):  $m/z$  770 [(OEP)Os(NO)(Me) + H] $^+$  (4), 739 [(OEP)Os(Me)] $^+$  (12). UV-vis spectrum ( $\lambda$  ( $\epsilon$ ,  $mM^{-1} cm^{-1}$ ),  $7.81 \times 10^{-6}$  M in  $CH_2Cl_2$ ): 351 (67), 445 (47), 552 (15), 584 (8) nm.

**(OEP)Os(NO)Cl.** Anal. Calcd for  $C_{36}H_{44}N_5O_2Cl$ : Cl, 4.50. Found: Cl, 4.36. IR ( $CH_2Cl_2$ ,  $cm^{-1}$ ):  $\nu_{NO}$  1799. IR (KBr,  $cm^{-1}$ ):  $\nu_{NO}$  1788 s; also 2966 w, 2932 w, 2870 w, 1468 m, 1446 m, 1373 w, 1316 w, 1272 m, 1154 m, 1111 w, 1057 m, 1020 s, 994 m, 964 m, 909 w, 800 w, 842 w.  $^1H$  NMR ( $CDCl_3$ ,  $\delta$ ): 10.41 (s, 4H, *meso*-H of OEP), 4.16 (m, 16H,  $CH_2CH_3$  of OEP), 2.02 (t,  $J = 8$ , 24H,  $CH_2CH_3$  of OEP). Low-resolution mass spectrum (FAB):  $m/z$  789 [(OEP)Os(NO)Cl] $^+$  (9), 754 [(OEP)Os(NO)] $^+$  (4). UV-vis spectrum ( $\lambda$  ( $\epsilon$ ,  $mM^{-1} cm^{-1}$ ),  $7.81 \times 10^{-6}$  M in  $CH_2Cl_2$ ): 349 (45), 366 (42), 432 (40), 544 (12), 579 (16) nm.

**(OEP)Os(NO)Br.** Anal. Calcd for  $C_{36}H_{44}N_5O_2Br$ : C, 51.92; H, 5.32; N, 8.41. Found: C, 51.72; H, 5.37; N, 8.05. IR ( $CH_2Cl_2$ ,  $cm^{-1}$ ):  $\nu_{NO}$  1796. IR (KBr,  $cm^{-1}$ ):  $\nu_{NO}$  1784 s; also 2967 m, 2933 w, 2869 w, 1468 w, 1444 w, 1273 w, 1155 m, 1112 w, 1057 w, 1020 m, 994 w, 964 w, 843 w.  $^1H$  NMR ( $CDCl_3$ ,  $\delta$ ): 10.41 (s, 4H, *meso*-H of OEP), 4.17 (m, 16H,  $CH_2CH_3$  of OEP), 2.02 (t,  $J = 8$ , 24H,  $CH_2CH_3$  of OEP). Low-resolution mass spectrum (FAB):  $m/z$  833 [(OEP)Os(NO)Br] $^+$  (9), 803 [(OEP)Os(Br)] $^+$  (3), 754 [(OEP)Os(NO)] $^+$  (6). UV-vis spectrum ( $\lambda$ ,  $CH_2Cl_2$ ): 351 (100, Soret), 369 (sh, 86), 439 (66), 548 (24), 583 (26) nm.

**[(OEP)Os(NO)] $_2(\mu-O)$ .** IR ( $CH_2Cl_2$ ,  $cm^{-1}$ ):  $\nu_{NO}$  1770 s. IR (KBr,  $cm^{-1}$ ):  $\nu_{NO}$  1760 s.  $^1H$  NMR ( $CDCl_3$ ,  $\delta$ ): 10.35 (s, 4H, *meso*-H of OEP), 4.15 (m, 16H,  $CH_2CH_3$  of OEP), 2.00 (t,  $J = 8$ , 24H,  $CH_2CH_3$  of OEP). Low-resolution mass spectrum (FAB):  $m/z$  771 [(OEP)Os(NO)(O) + H] $^+$  (50), 754 [(OEP)Os(NO)] $^+$  (100), 724 [(OEP)Os] $^+$  (15). UV-vis spectrum ( $\lambda$  ( $\epsilon$ ,  $mM^{-1} cm^{-1}$ ),  $7.81 \times 10^{-6}$  M in  $CH_2Cl_2$ ): 341 (75), 419 (186), 533 (33), 568 (54) nm.

**(TTP)Os(NO)Me.** IR ( $CH_2Cl_2$ ,  $cm^{-1}$ ):  $\nu_{NO}$  1729. IR (KBr,  $cm^{-1}$ ):  $\nu_{NO}$  1732 m; also 3023 w, 2953 w, 2923 w, 2873 w, 1528 w, 1512 w, 1496 w, 1446 w, 1351 m, 1306 m, 1212 m, 1179 m, 1105 w, 1069 m, 1016 s, 796 s, 718 m, 525 m.  $^1H$  NMR ( $CDCl_3$ ,  $\delta$ ): 8.89 (s, 8H, *pyr*-H of TTP), 8.15 (d,  $J = 7$ , 4H, *o*-H of TTP), 8.06 (d,  $J = 8$ , 4H, *o'*-H of TTP), 7.55 (app t,  $J = 7/8$ , 8H, *m*-H of TTP), 2.70 (s, 12H,  $CH_3$  of TTP), -7.35 (s, 3H, *Me*). UV-vis spectrum ( $\lambda$  ( $\epsilon$ ,  $mM^{-1} cm^{-1}$ ),  $1.44 \times 10^{-5}$  M in  $CH_2Cl_2$ ): 345 (sh, 44), 361 (46), 408 (45), 454 (91), 573 (13), 616 (12) nm.

**(OEP)Os(NO)(*p*- $C_6H_4F$ ).** IR ( $CH_2Cl_2$ ,  $cm^{-1}$ ):  $\nu_{NO}$  1748. IR (KBr,  $cm^{-1}$ ):  $\nu_{NO}$  1746 s; also 2965 m, 2932 w, 2868 w, 1574 w, 1483 m, 1466 w, 1446 w, 1372 w, 1318 w, 1272 m, 1224 m, 1161 m, 1153 m, 1112 w, 1056 m, 1020 m, 993 m, 962 w, 841 w, 813 m, 746 w, 727 w, 716 w, 567 w, 501 w.  $^1H$  NMR ( $CDCl_3$ ,  $\delta$ ): 10.24 (s, 4H, *meso*-H of OEP), 4.22 (m, 2H, *m*-H of *p*- $C_6H_4F$ , overlapping with OEP), 4.12 (m, 16H,  $CH_2CH_3$  of OEP), 1.96 (t,  $J = 8$ , 24H,  $CH_2CH_3$  of OEP), -0.29 (t,  $J = 8$ , 2H, *o*-H of *p*- $C_6H_4F$ ). Low-resolution mass spectrum (FAB):  $m/z$  819 [(OEP)Os(*p*- $C_6H_4F$ )] $^+$  (12). UV-vis spectrum ( $\lambda$ , benzene): 352 (Soret), 443, 552, 585 nm.

**(OEP)Os(*t*-Bu) $_2$ .**  $^1H$  NMR ( $CDCl_3$ ,  $\delta$ ): 9.03 (s, 4H, *meso*-H of OEP), 3.93 (q,  $J = 8$ , 16H,  $CH_2CH_3$  of OEP), 1.80 (t,  $J = 8$ , 24H,  $CH_2CH_3$  of OEP), -3.18 (s, 9H, *t*-Bu).

**(OEP)Os(Et) $_2$ .**  $^1H$  NMR ( $CDCl_3$ ,  $\delta$ ): 9.23 (s, 4H, *meso*-H of OEP), 3.67 (q,  $J = 8$ , 16H,  $CH_2CH_3$  of OEP), 1.73 (t,  $J = 8$ , 24H,  $CH_2CH_3$  of OEP), -0.72 (q,  $J = 7$ , 4H,  $CH_2CH_3$  of Et), -4.77 (t,  $J = 7$ , 6H,  $CH_2CH_3$  of Et).

**(OEP)Os(Me) $_2$ .**  $^1H$  NMR ( $CDCl_3$ ,  $\delta$ ): 9.34 (s, 4H, *meso*-H of OEP), 3.70 (q, 16H,  $J = 8$ ,  $CH_2CH_3$  of OEP), 1.74 (t,  $J = 8$ , 24H,  $CH_2CH_3$  of OEP), -1.16 (s, 6H,  $CH_3$ ). UV-vis spectrum ( $\lambda$ , benzene): 330 (72), 371 (100, Soret), 394 (sh, 68), 440 (39), 547 (17) nm.

**(OEP)Os(*p*- $C_6H_4F$ ) $_2$ .** IR (KBr,  $cm^{-1}$ ): 2964 w, 2929 w, 2869 w, 1567 w, 1474 w, 1453 w, 1262 w, 1222 m, 1158 m, 1108 w, 1055 w, 1018 m, 812 m.  $^1H$  NMR ( $CDCl_3$ ,  $\delta$ ): 9.71 (s, 4H, *meso*-H of OEP), 5.05 (t,  $J = 9$ , 4H, *p*- $C_6H_4F$ ), 3.91 (q,  $J = 8$ , 16H,  $CH_2CH_3$  of OEP), 1.75 (t,  $J = 8$ , 24H,  $CH_2CH_3$  of OEP), 1.15 (m, 4H, *p*- $C_6H_4F$ ). Low-resolution mass spectrum (FAB):  $m/z$  914 [(OEP)Os(*p*- $C_6H_4F$ ) $_2$ ] $^+$  (4), 819 [(OEP)Os(*p*- $C_6H_4F$ )] $^+$  (42). UV-vis ( $\lambda$ ,  $CH_2Cl_2$ ): 368 (100, Soret), 493 (26), 641 (13) nm. UV-vis ( $\lambda$ , benzene): 369 (100, Soret), 489 (28), 641 (16) nm.

**Synthesis of (OEP)Os(NO)F.<sup>63</sup> Method I.** To a stirred solution of (OEP)Os(NO)Cl (0.009 g, 0.011 mmol) in toluene (10 mL) was added excess  $AgBF_4$  (0.010 g, 0.051 mmol). The red color of the solution gradually deepened. Silica gel TLC (1:1  $CH_2Cl_2$ /hexane) indicated that the reaction was complete in 30 min. The reaction solution was directly transferred onto the top of an alumina column (2  $\times$  40 cm) prepared in hexane. Elution with  $CH_2Cl_2$  under nitrogen generated a red band, which was collected. Solvent removal gave (OEP)Os(NO)F (0.008 g, 92% isolated yield). IR ( $CH_2Cl_2$ ,  $cm^{-1}$ ):  $\nu_{NO}$  1795. IR (KBr,  $cm^{-1}$ ):  $\nu_{NO}$  1784 s; also 2968 m, 2934 w, 2870 w, 1469 w, 1447 w, 1373 w, 1273 w, 1155 m, 1111 w, 1056 w, 1020 m, 994 w, 964 w, 843 w, 745 w, 716 w, 555 w.  $^1H$  NMR ( $CDCl_3$ ,  $\delta$ ): 10.40 (s, 4H, *meso*-H of OEP), 4.17 (m, 16H,  $CH_2CH_3$  of OEP), 2.00 (t,  $J = 8$ , 24H,  $CH_2CH_3$  of OEP). Low-resolution mass spectrum (FAB):  $m/z$  773 [(OEP)Os(NO)F] $^+$  (100), 754 [(OEP)Os(NO)] $^+$  (53), 743 [(OEP)Os(F)] $^+$  (8). UV-vis spectrum ( $\lambda$ ,  $CH_2Cl_2$ ): 339 (36), 417 (100, Soret), 533 (18), 568 (33) nm.

**Method II.** To a stirred solution of (OEP)Os(CO) (0.020 g, 0.027 mmol) in  $CH_2Cl_2$  (10 mL) was added excess  $NOPF_6$  (0.010 g, 0.057 mmol). The reaction mixture was stirred at room temperature for 1 h, and silica gel TLC ( $CH_2Cl_2$ ) indicated that all the starting material had been consumed. The volume of the solution was then reduced to ca. 2 mL under vacuum, and the solution was transferred onto an alumina column (2  $\times$  40 cm) prepared in hexane. Elution with  $CH_2Cl_2$  under nitrogen gave a red band from which (OEP)Os(NO)F was isolated (0.003 g, 14% isolated yield). The [(OEP)Os(NO)] $_2(\mu-O)$  compound was also obtained by eluting the remaining residue with a 1:1 ratio of THF/hexane (0.003 g, 15% isolated yield based on Os). Some other unidentified products remained on the column, and they were eluted with THF.

**Preparation of (OEP)Os(NS)Cl.** To a THF (25 mL) solution of (OEP)Os(CO) (0.060 g, 0.080 mmol) was added excess  $(NSCl)_3$  (0.014 g, 0.057 mmol). The mixture was heated to reflux for 30 min. The color of the solution changed from red to brown, then to green. All the solvent was then removed, the green solid was purified by neutral alumina chromatography with  $CH_2Cl_2$  as eluent. The green fraction was collected, and all the solvent was removed. The green residual solid was further purified by recrystallization from  $CH_2Cl_2$ /hexane at -20  $^\circ C$  to give (OEP)Os(NS)Cl $\cdot$ 0.9 $CH_2Cl_2$  (0.034 g, 0.039 mmol, 49% yield). IR (KBr,  $cm^{-1}$ ):  $\nu_{NS}$  1270 s; also 2967 w, 2930 w, 2869 w, 1470 m, 1444 m, 1372 w, 1362 w, 1317 w, 1226 w, 1152 s, 1111 m, 1054 m, 1020 s, 994 m, 963 m, 839 m, 744 s, 714 m.  $^1H$  NMR ( $C_6D_6$ ,  $\delta$ ): 10.65 (s, 4H, *meso*-H of OEP), 4.26 (s,  $CH_2Cl_2$ ), 4.00 (q,  $J = 8$ , 16H,  $CH_2CH_3$  of OEP), 1.90 (t,  $J = 8$ , 24H,  $CH_2CH_3$  of OEP).  $^1H$  NMR ( $CDCl_3$ ,  $\delta$ ): 10.49 (s, 4H,

Table 1. Crystal Data and Structure Refinement

	[(OEP)Os(NO)] <sub>2</sub> ( $\mu$ -O)·2HCl	(OEP)Os(NS)Cl	(OEP)Os(NS)Me
formula	C <sub>72</sub> H <sub>90</sub> N <sub>10</sub> O <sub>3</sub> Cl <sub>2</sub> Os <sub>2</sub>	C <sub>36</sub> H <sub>44</sub> N <sub>5</sub> ClSOs	C <sub>37</sub> H <sub>47</sub> N <sub>5</sub> SOs
fw	1594.84	804.47 <sup>c</sup>	784.06
T, K	188(2)	173(2)	188(2)
cryst syst	tetragonal	monoclinic	triclinic
space group	<i>P4/nnc</i>	<i>P2<sub>1</sub></i>	<i>P1</i>
unit cell dimens	<i>a</i> = 13.8263(9) Å, $\alpha$ = 90° <i>b</i> = 13.8263(9) Å, $\beta$ = 90° <i>c</i> = 17.342(2) Å, $\gamma$ = 90°	<i>a</i> = 8.3150(11) Å, $\alpha$ = 90° <i>b</i> = 21.184(3) Å, $\beta$ = 103.459(9)° <i>c</i> = 10.8990(14) Å, $\gamma$ = 90°	<i>a</i> = 8.631(2) Å, $\alpha$ = 81.45(3)° <i>b</i> = 10.344(4) Å, $\beta$ = 67.73(2)° <i>c</i> = 10.504(4) Å, $\gamma$ = 68.92(2)°
<i>V</i> , Z	3315.2(5) Å <sup>3</sup> , 2	1867.1(5) Å <sup>3</sup> , 2	809.7(5) Å <sup>3</sup> , 1
<i>D</i> (calcd), g/cm <sup>3</sup>	1.598	1.431	1.608
abs coeff, mm <sup>-1</sup>	3.966	3.572	4.037
<i>F</i> (000)	1604	808	396
cryst size, mm	0.18 × 0.38 × 0.22	0.40 × 0.32 × 0.03	0.12 × 0.34 × 0.19
$\theta$ range for data collection, deg	1.88–24.99	1.92–25.04	2.10–25.00
index ranges	0 ≤ <i>h</i> ≤ 16, -13 ≤ <i>k</i> ≤ 11, -20 ≤ <i>l</i> ≤ 0	-9 ≤ <i>h</i> ≤ 9, -25 ≤ <i>k</i> ≤ 22, 0 ≤ <i>l</i> ≤ 12	-9 ≤ <i>h</i> ≤ 0, -12 ≤ <i>k</i> ≤ 11, -12 ≤ <i>l</i> ≤ 11
no. of reflns collected	2375	9496	2986
no. of indep reflns	1475 [ <i>R</i> (int) = 0.0389]	5286 [ <i>R</i> (int) = 0.0256]	2768 [ <i>R</i> (int) = 0.0213]
abs corr	semiempirical from $\psi$ -scans	SADABS	semiempirical from $\psi$ -scans
max and min transmission	0.1412 and 0.0944	1.000 and 0.540	0.5263 and 0.3883
data/restraints/params	1474/0/110	5285/30/435	2763/1/195
goodness-of-fit on <i>F</i> <sup>2</sup>	1.053	1.049	1.087
final <i>R</i> indices	<i>R</i> 1 = 0.0346, w <i>R</i> 2 = 0.0746	<i>R</i> 1 = 0.0334, w <i>R</i> 2 = 0.0871	<i>R</i> 1 = 0.0636, w <i>R</i> 2 = 0.1546
[ <i>I</i> > 2 $\sigma$ ( <i>I</i> )] <sup>a,b</sup>			
<i>R</i> indices (all data) <sup>a,b</sup>	<i>R</i> 1 = 0.0615, w <i>R</i> 2 = 0.0875	<i>R</i> 1 = 0.0348, w <i>R</i> 2 = 0.0900	<i>R</i> 1 = 0.0643, w <i>R</i> 2 = 0.1562
largest diff peak and hole, e Å <sup>-3</sup>	0.846 and -0.790	1.868 and -1.046	2.602 and -2.481

<sup>a</sup> *R*1 =  $\sum ||F_o| - |F_c|| / \sum |F_o|$ . <sup>b</sup> w*R*2 =  $\{\sum [w(F_o^2 - F_c^2)^2] / \sum [wF_o^4]\}^{1/2}$ . <sup>c</sup> The crystal contains an unidentified solvent molecule (see Experimental Section).

*meso*-H of OEP), 5.28 (s, CH<sub>2</sub>Cl<sub>2</sub>), 4.20 (q, *J* = 8, 16H, CH<sub>3</sub>CH<sub>2</sub> of OEP), 2.03 (t, *J* = 8, 24H, CH<sub>3</sub>CH<sub>2</sub> of OEP). Low-resolution mass spectrum (FAB): *m/z* 805 [(OEP)Os(NS)Cl]<sup>+</sup> (58), 770 [(OEP)Os(NS)]<sup>+</sup> (53). UV-vis spectrum ( $\lambda$  ( $\epsilon$ , mM<sup>-1</sup> cm<sup>-1</sup>), 1.24 × 10<sup>-5</sup> M in CH<sub>2</sub>Cl<sub>2</sub>): 362 (75), 385 (sh, 63), 605 (6) nm. Attempts to obtain an elementally pure sample of this air-sensitive sample have so far not been very successful. Anal. Calcd for C<sub>36</sub>H<sub>44</sub>N<sub>5</sub>ClSOs·0.9CH<sub>2</sub>Cl<sub>2</sub>: C, 50.31; H, 5.24; N, 7.95; Cl, 11.27; S, 3.64. Found: C, 49.54; H, 5.13; N, 7.75; Cl, 10.84; S, 3.71.

**(OEP)Os(<sup>15</sup>NS)Cl.** This compound was prepared similarly to the unlabeled analogue (using (<sup>15</sup>NSCl)<sub>3</sub>). IR (KBr, cm<sup>-1</sup>):  $\nu^{15$ NS 1231 s.

**Synthesis of (OEP)Os(NS)Me.** To a solution of (OEP)Os(NS)Cl (0.031 g, 0.038 mmol) in THF (10 mL) was added MeMgBr (0.20 mL, 1.4 M in THF, 0.28 mmol) dropwise at room temperature. The color of the solution changed from green to brown-red, and the solvent was removed in vacuo immediately. The resulting brown residue was dissolved in benzene and chromatographed (under reduced laboratory lighting) under nitrogen on an alumina column (2 × 60 cm) prepared in hexane. Elution with a 1:1 mixture of benzene/hexane gave a brown band, which was collected and taken to dryness to give (OEP)Os(Me)<sub>2</sub> (0.004 g, 14% isolated yield).

A second light-green band was collected and taken to dryness in vacuo to give (OEP)Os(NS)Me (0.007 g, 23% isolated yield). IR (KBr, cm<sup>-1</sup>):  $\nu$ NS 1196 m; also 2966 s, 2930 m, 2869 w, 1470 w, 1444 w, 1372 w, 1317 w, 1272 m, 1226 w, 1151 m, 1111 w, 1055 m, 1020 s, 994 m, 963 m, 838 w, 745 m, 713 w. <sup>1</sup>H NMR (CDCl<sub>3</sub>,  $\delta$ ): 10.30 (s, 4H, *meso*-H of OEP), 4.14 (m, 16H, CH<sub>2</sub>CH<sub>3</sub> of OEP), 1.97 (t, *J* = 8, 24H, CH<sub>2</sub>CH<sub>3</sub> of OEP), -7.88 (s, 3H, CH<sub>3</sub>). UV-vis spectrum ( $\lambda$ , CH<sub>2</sub>Cl<sub>2</sub>): 372 (100, Soret), 433 (br sh, 26), 585 (br sh, 12) nm.

**(OEP)Os(<sup>15</sup>NS)Me.** This compound was prepared similarly to the unlabeled analogue. IR (KBr, cm<sup>-1</sup>):  $\nu^{15$ NS 1163.

**Solid-State Structural Determinations.** Details of crystal data and refinement are given in Table 1. The crystal data were collected using Mo K $\alpha$  ( $\lambda$  = 0.710 73 Å) radiation.

**(i) [(OEP)Os(NO)]<sub>2</sub>( $\mu$ -O)·2HCl.** A suitable crystal of the compound (obtained from the reaction of ClNO with (OEP)-

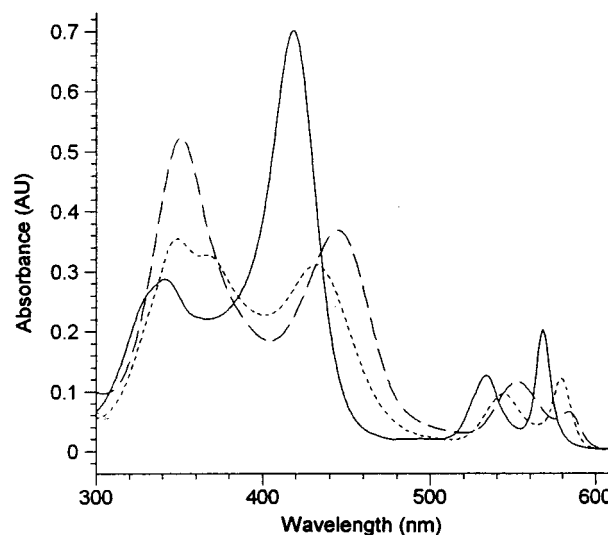


**Figure 1.** UV-vis spectra of [(OEP)Os(NO)]<sub>2</sub>( $\mu$ -O) (—), (OEP)Os(NO)Me (---), and (OEP)Os(NO)Cl (···) in CH<sub>2</sub>Cl<sub>2</sub>. [(OEP)Os— concentration of 7.81 × 10<sup>-6</sup> M.]

Os(CO), see above) for a single-crystal X-ray structural determination was grown by slow solvent evaporation from saturated CH<sub>2</sub>Cl<sub>2</sub> solution under nitrogen for 3 days. The crystal data were collected on a Siemens P4 diffractometer. The data were corrected for Lorentz and polarization effects, and an empirical absorption correction based on  $\psi$ -scans was applied. The structure was solved by the direct method using the SHELXTL (Siemens) system and refined by full-matrix least-squares based on *F*<sup>2</sup> using all reflections. The hydrogen atom of the HCl molecule (H1) was located in the difference map and refined isotropically. All the other hydrogen atoms were included with idealized parameters. The unit cell contains two [(OEP)Os(NO)]<sub>2</sub>( $\mu$ -O) and four HCl molecules, and they pack along the 4-fold axis in alternate layers of hydrogen-bonded HCl and [(OEP)Os(NO)]<sub>2</sub>( $\mu$ -O) molecules as shown in Figure

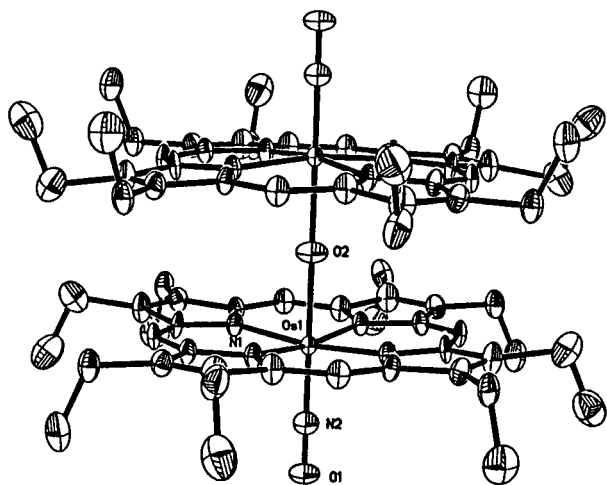


**Figure 2.** Molecular structure of  $[(\text{OEP})\text{Os}(\text{NO})_2(\mu\text{-O})]$  showing 30% ellipsoids. Hydrogen atoms have been omitted for clarity.

4a.<sup>57</sup> There are actually eight sites of the HCl molecule in the unit cell, with each site occupied only 50%, thus generating a total of four HCl molecules. The  $[(\text{OEP})\text{Os}(\text{NO})_2(\mu\text{-O})]$  molecule has a very high crystallographically imposed symmetry with only one-eighth of the molecule being unique. Several atoms are situated at special symmetry sites. The O2 atom has the highest point symmetry and is located at special position  $a\ 42$  symmetry point. The Os1, O1, and N2 atoms lie along the 4-fold symmetry axis, and the C11 and H1 atoms also lie along the 2-fold axis. For the HCl molecule, the sites are occupied only 50% and both the C11 and H1 atoms were refined with a 0.25 occupancy factor instead of 0.5, which is required for these special positions.

(ii) **(OEP)Os(NS)Cl.** A suitable crystal for structural determination was grown by slow solvent evaporation from the  $\text{CH}_2\text{Cl}_2$  solution in a drybox. The single-crystal X-ray structural analysis was performed at the University of Minnesota. The crystal data were collected on a Siemens SMART Platform CCD instrument. The space group was determined based on systematic absences and intensity statistics. A successful direct-methods solution was calculated which provided most non-hydrogen atoms from the  $E$ -map. Several full-

(57) One reviewer suggested that the Cl atoms could be from  $\text{CH}_2\text{-Cl}_2$  molecules, which would be consistent with the observed Cl...Cl distance of 2.85 Å. The reviewer also suggested that HCl (strong acid) might not be expected to coexist with the  $\mu$ -oxo dimer in the same crystal. We checked these points by reexamination of the crystallography (a) and by chemical means (b). (a) It seems highly unlikely that  $\text{CH}_2\text{Cl}_2$  is present, since the close proximity of the 4-fold symmetry axis will generate eight possible Cl-atom sites rather than the four which were observed. A close reexamination of the difference map shows absolutely no indication of the presence of a carbon atom, even at fractional occupancy. We feel that the presence of HCl in the lattice as described is consistent with the observed data. (b) Interestingly, HCl (which was present in the ClNO solution used to form the mixture of  $(\text{OEP})\text{Os}(\text{NO})\text{Cl}$  and  $[(\text{OEP})\text{Os}(\text{NO})_2(\mu\text{-O})]$ ) reacts only very slowly with the oxo dimer in  $\text{CH}_2\text{Cl}_2$ , even at room temperature under nitrogen. For example, stirring a 1:3 mixture of the oxo dimer and HCl-Et<sub>2</sub>O (Aldrich) over a 23 h period results in no observable reaction (as determined by UV-vis spectroscopy). A further examination of the reaction solution by TLC (silica gel) *in air* revealed only trace formation of  $(\text{OEP})\text{Os}(\text{NO})\text{Cl}$ . Reaction of  $[(\text{OEP})\text{Os}(\text{NO})_2(\mu\text{-O})]$  with 10 equiv of HCl-Et<sub>2</sub>O for 1 h results in a very small red shift of the peaks in the UV-vis spectrum. However, only  $[(\text{OEP})\text{Os}(\text{NO})_2(\mu\text{-O})]$  is recovered after removal of the solvent and washing the resulting residue with hexane, indicating lack of formation of  $(\text{OEP})\text{Os}(\text{NO})\text{Cl}$ . Reaction of this 1:10 mixture for 18 h, however, results in ca. 40% conversion to  $(\text{OEP})\text{Os}(\text{NO})\text{Cl}$ . In summary, we note that under our crystallization conditions, the reaction of  $[(\text{OEP})\text{Os}(\text{NO})_2(\mu\text{-O})]$  with 2–6 equiv of HCl is slow enough to allow HCl and the oxo dimer to coexist in the same crystal. It thus appears that the two axial  $\pi$ -acid NO ligands are able to withdraw sufficient electron density from the  $\mu$ -oxo bridge to render it less reactive to HCl than would otherwise have been expected.

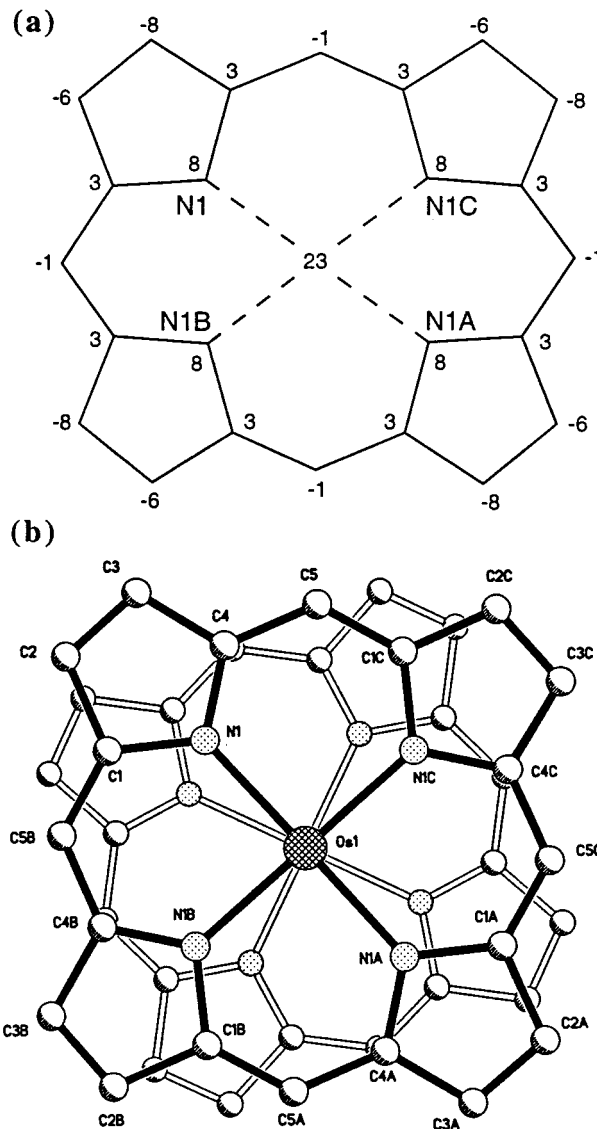


**Figure 3.** (a) Perpendicular atom displacements (in units of 0.01 Å) of the porphyrin core from the 24-atom mean porphyrin plane. Positive values are toward the axial NO ligand. (b) View of the porphyrin core orientations relative to each other, with the view along the Os–Os direction.

matrix least-squares/difference Fourier cycles were performed, which located the remainder of the non-hydrogen atoms. All non-hydrogen atoms were refined with anisotropic displacement parameters. All hydrogen atoms were placed in ideal positions and refined as riding atoms with relative isotropic displacement parameters. The structure was as expected, but the axial Cl and NS ligands are disordered in a 0.81:0.19 ratio. The space group is  $P2_1$  and appears to have a minor inversion twin component in a 0.91:0.09 ratio. Early work found disordered solvent occupying  $230.7 \text{ \AA}^3$  out of a unit cell volume of  $1867.1 \text{ \AA}^3$  or 12.3% of the total. PLATON<sup>58</sup>/SQUEEZE was used to correct the data for the effects of disordered solvent. Residuals improved about 1% while identifying 99 electrons worth of scattering in this void. It is very likely that this solvent is hexane, but the smeared-out positions made this impossible to refine. Thus, the stated empirical formula,  $F_{000}$ , formula weight, absorption coefficient, etc., should be taken with caution since no solvent was taken into consideration in their calculation. Finally, the axial Cl/NS disorder forced the use of several positional and anisotropic displacement param-

(58) Spek, A. L. *Acta Crystallogr.* **1990**, *A46*, C34.

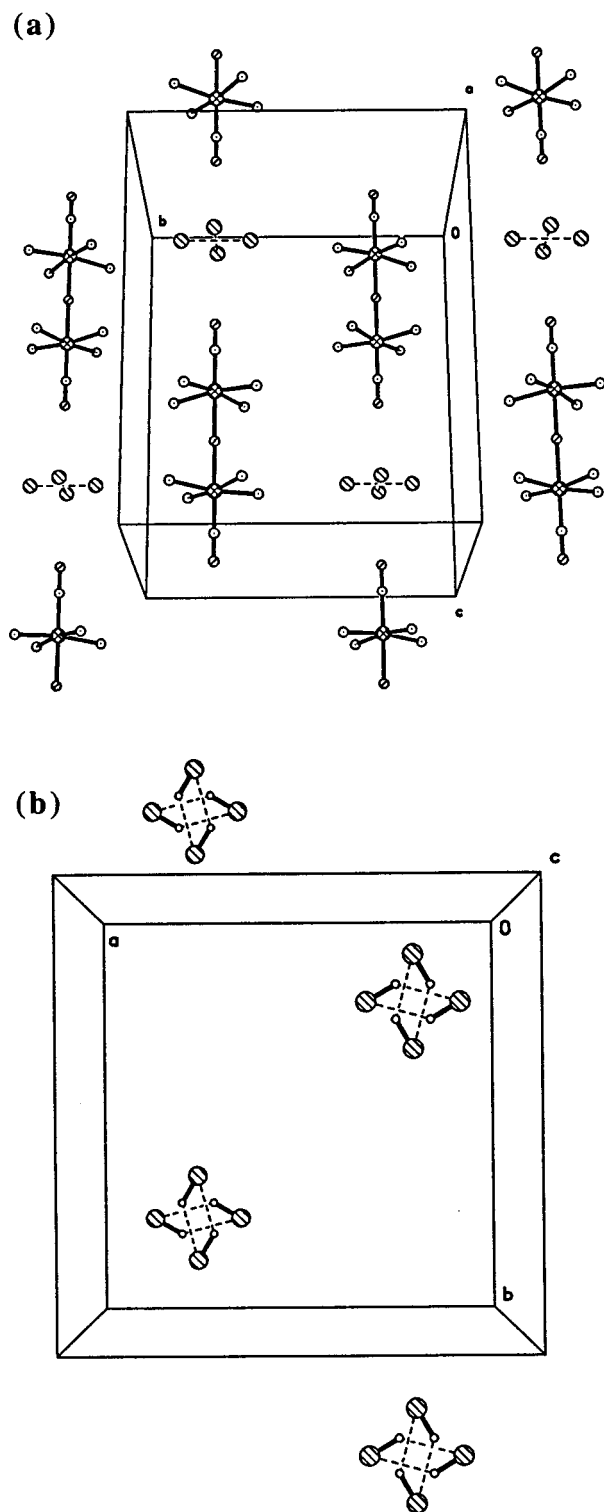


**Figure 4.** (a) View of the unit cell containing  $[(\text{OEP})\text{Os}(\text{NO})]_2(\mu\text{-O})\cdot 2\text{HCl}$ . (b) View of the alternate pairs of HCl molecules showing the H-bond interactions.

eter restraints. Thirty restraints (SHELXTL SAME/SADI/ISOR) were applied to these atoms and to N1/C1. N1/C1 had uncharacteristic elongated thermal ellipsoids normal to the porphyrin ring. The anisotropic displacement parameters for C1 were nonpositive definite without the restraint. Least-squares correlations were checked for these atoms, but none involving these atoms were found.

**(iii) (OEP)Os(NS)Me.** A suitable crystal of (OEP)Os(NS)(Me) for structural determination was grown by slow solvent evaporation from a  $\text{CH}_2\text{Cl}_2$  solution under nitrogen. The

crystal data were collected on a Siemens P4 diffractometer. The data were corrected for Lorentz and polarization effects, and an empirical absorption correction based on  $\psi$ -scans was applied. The structure was solved by the heavy-atom method using the SHELXTL (Siemens) system and refined by full-matrix least-squares based on  $F^2$  using all reflections. Hydrogen atoms were included with idealized parameters. Hydrogen atoms were not included for C37A, which was affected by disorder. The molecule has rigorous crystallographic inversion symmetry, hence the asymmetric unit contains only one-half of the unique molecule. The Os atom lies at the center of symmetry. Because of the crystallographic symmetry requirement, the axial methyl (C37A or C37) and NS (N3 and S1) groups are completely disordered. Attempts to refine C37 and N3 with slightly different positional parameters yielded poor and unstable refinement. Finally, C37 and N3 were assigned identical positional and thermal parameters, which gave a more stable refinement. All the non-hydrogen atoms were refined anisotropically except C37, N3, and S1 (the atoms affected by the disorder), which were refined isotropically. The sulfur atom was also refined anisotropically and did not show any alternate sulfur-atom position. There are several large peaks in the vicinity, but none of them are consistent with an alternate sulfur-atom position. We feel that the large thermal parameter for the sulfur atom is due to the general disorder, and because of the limitations of the data and the disorder problem, it is appropriate to refine it isotropically. The possibility of NO contamination is also ruled out on the basis of chemical evidence.

The structure was also solved and refined in the  $P\bar{1}$  (No. 1) alternate space group, since it will not have the disordered methyl and NS groups. However, it always gave peaks of the NS group on both sides of the porphyrin plane and gave extremely poor and unstable refinement. Therefore, the choice of  $P\bar{1}$  space group was deemed to be correct. In addition to the disorder, the overall quality of the data and refinement is limited (slightly large  $R$  factor and residual peaks in the difference map) due to poor quality crystals. All the crystals obtained from different crystallization methods were extremely fragile and unstable. Repeated attempts to grow better quality crystals were unsuccessful.

## Results and Discussion

The organometallic (OEP)Os(NO)R complexes are formed from the reaction of (OEP)Os(CO) with  $\text{NOPF}_6$  in  $\text{CH}_2\text{Cl}_2$ , followed by reaction of the  $[(\text{OEP})\text{Os}(\text{NO})]\text{-PF}_6$  intermediate with  $\text{RMgX}$  ( $\text{X} = \text{Cl}, \text{Br}$ ) in THF. Although the (OEP)Os(NO)R complexes were the initial target products, we found that other nitrosyl and non-nitrosyl products were also formed in this reaction of  $[(\text{OEP})\text{Os}(\text{NO})]\text{PF}_6$  with Grignard reagents.<sup>59</sup> The general reaction is shown in Scheme 1.

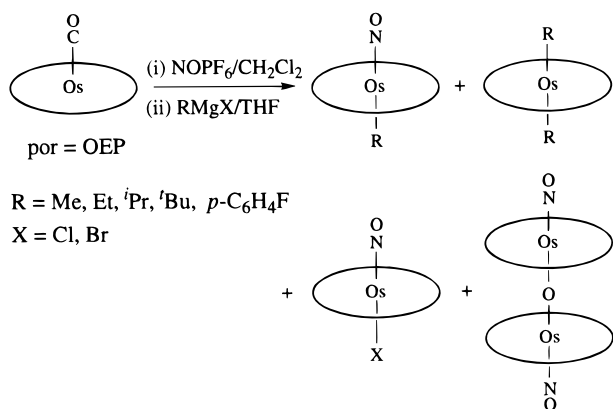
The initial reaction to produce  $[(\text{OEP})\text{Os}(\text{NO})]\text{PF}_6$  is performed in  $\text{CH}_2\text{Cl}_2$  at room temperature under reduced laboratory lighting (see later) with the rigorous exclusion of air and moisture to avoid the formation of the (OEP)Os(NO)( $\text{O}_2\text{PF}_2$ ) hydrolysis product.<sup>60</sup> The Grignard reaction is performed in THF, and the progress of the reaction is monitored by TLC (silica gel) using a 1:1 benzene/hexane mixture in air.

The products (Scheme 1) are then separated by column chromatography on neutral alumina using a 1:1

(59) The reaction of  $\text{RMgX}$  with non-nitrosyl osmium- and other metalloporphyrin cations to produce organometallic derivatives has some precedent, see: (a) Reference 43. (b) Ogoshi, H.; Sugimoto, H.; Yoshida, Z.-I.; Kobayashi, H.; Sakai, H.; Maeda, Y. *J. Organomet. Chem.* **1982**, *234*, 185–195.

(60) Chen, L.; Khan, M. A.; Richter-Addo, G. B. *Inorg. Chem.* **1998**, *37*, 533–540.

Scheme 1



benzene/hexane mixture as eluent. The (OEP)Os(R)<sub>2</sub> compound is eluted first followed by the (OEP)Os(NO)R nitrosyl compound. The (OEP)Os(NO)X nitrosyl halide is eluted next with CH<sub>2</sub>Cl<sub>2</sub>/hexane, and finally the [(OEP)Os(NO)]<sub>2</sub>(μ-O) oxo dimer is eluted with THF/hexane. The chromatography is performed under reduced lighting to minimize the decomposition of the nitrosyl alkyl/aryl products. The nitrosyl compounds have been characterized by IR and <sup>1</sup>H NMR spectroscopy, FAB mass spectrometry, and by elemental analyses. They have also been characterized by UV-vis spectroscopy, and representative spectra are shown in Figure 1.

The formation of the (OEP)Os(R)<sub>2</sub> compound probably arises from further reaction of (OEP)Os(NO)R with RMgX. Indeed, the reaction of a pure sample of (OEP)Os(NO)(*p*-C<sub>6</sub>H<sub>4</sub>F) with excess (*p*-C<sub>6</sub>H<sub>4</sub>F)MgBr for 2 h results in a 20% conversion of the nitrosyl compound to the non-nitrosyl (OEP)Os(*p*-C<sub>6</sub>H<sub>4</sub>F)<sub>2</sub> derivative (50% conversion after 24 h). A similar nitrosyl-for-alkyl substitution has been noted for the analogous (TTP)-Ru(NO)(*p*-C<sub>6</sub>H<sub>4</sub>F) compound.<sup>44</sup> The formation of (OEP)Os(NO)X from RMgX was unexpected, however, since the reaction of [(OEP)Os(NO)]PF<sub>6</sub> with MgCl<sub>2</sub> or KBr under refluxing conditions in THF does not, at least in our hands, produce the (OEP)Os(NO)X compounds. The novel [(OEP)Os(NO)]<sub>2</sub>(μ-O) oxo dimer product probably arises from some (OEP)Os(CO)(H<sub>2</sub>O) or from adventitious air and moisture during the reaction and isolation procedures. Indeed, a quantitative conversion of (OEP)Os(NO)(<sup>*t*</sup>Bu) to [(OEP)Os(NO)]<sub>2</sub>(μ-O) occurs within 45 min (as monitored by UV-vis spectroscopy) when a CH<sub>2</sub>Cl<sub>2</sub> solution of an authentic sample of (OEP)Os(NO)(<sup>*t*</sup>Bu) is exposed to air.

**Nitrosyl Alkyl/Aryl Complexes.** The red (OEP)Os(NO)R complexes are isolated in 5–44% yields depending on the reaction conditions and the nature of R. The nitrosyl products appear to be moderately stable in air as solids for short periods (hours). However, their solutions are sensitive to air and moisture and to laboratory lighting: their benzene solutions being more stable than their CH<sub>2</sub>Cl<sub>2</sub> solutions. In general, the observed order of stability of these nitrosyl products is (OEP)Os(NO)Me > (OEP)Os(NO)Et > (OEP)Os(NO)(<sup>*i*</sup>Pr) > (OEP)Os(NO)(<sup>*t*</sup>Bu).

These (OEP)Os(NO)R compounds are of the {Os(NO)}<sup>6</sup> formulation according to the Enemark–Feltham

notation<sup>61</sup> and are expected to have linear Os–NO linkages. Although we have not been able to grow suitable crystals of any of these organoosmium nitrosyls for an X-ray diffraction study, we note that the  $\nu_{\text{NO}}$  range in the IR spectra of these complexes (1703–1748 cm<sup>-1</sup>) is lower than those for (OEP)Os(NO)(S-*i*-C<sub>5</sub>H<sub>11</sub>) (1757 cm<sup>-1</sup>) and (OEP)Os(NO)(O-*n*-Bu) (1757 cm<sup>-1</sup>) but are substantially lower than that displayed for the cationic Os–NO center in (OEP)Os(NO)(O<sub>2</sub>PF<sub>2</sub>) (1820 cm<sup>-1</sup>). Several of these latter (OEP)Os(NO)-containing derivatives display linear Os–NO fragments in their solid-state structures.<sup>60</sup>

The IR  $\nu_{\text{NO}}$  of these compounds decrease in the order (OEP)Os(NO)(*p*-C<sub>6</sub>H<sub>4</sub>F) (1748 cm<sup>-1</sup>) > (OEP)Os(NO)-Me (1720 cm<sup>-1</sup>) > (OEP)Os(NO)Et (1710 cm<sup>-1</sup>) > (OEP)Os(NO)(<sup>*i*</sup>Pr) (1703 cm<sup>-1</sup>) ≈ (OEP)Os(NO)(<sup>*t*</sup>Bu) (1703 cm<sup>-1</sup>) and generally reflects the electron-donating abilities of the R ligands and the ability of the trans  $\pi$ -acid NO ligand to effectively withdraw additional electron density from the metal center in these complexes. The  $\nu_{\text{NO}}$  of the tetraarylporphyrin (TTP)Os(NO)-Me complex is at 1729 cm<sup>-1</sup> and reflects the fact that the (TTP)Os fragment is less electron rich than the (OEP)Os fragment.<sup>62</sup>

The <sup>1</sup>H NMR spectra of these (OEP)Os(NO)R complexes are consistent with their formulation. In an excellent review on cis- and trans-effects/influences in metalloporphyrins, Buchler has shown that the  $\delta_{\text{meso}}$  peak in (OEP)Os complexes is a measure of the overall back-bonding ability of the Os center to the porphyrin.<sup>62</sup> In general, a more electron-rich Os center will result in an upfield shift of  $\delta_{\text{meso}}$ . The  $\delta_{\text{meso}}$  peaks (of the OEP macrocycle) in these (OEP)Os(NO)R complexes fall within the narrow 10.21–10.24 ppm range, although significant changes are observed in  $\nu_{\text{NO}}$ . Consequently, and not unexpectedly, it appears that the trans-influence involving the axial ligand interactions is larger than the cis-influence in the (OEP)Os(NO)R complexes. Indeed, our observation that the  $\delta_{\text{meso}}$  peaks for the non-nitrosyl (OEP)Os(R)<sub>2</sub> complexes decrease significantly in the order (OEP)Os(*p*-C<sub>6</sub>H<sub>4</sub>F)<sub>2</sub> (9.71 ppm) > (OEP)Os(Me)<sub>2</sub> (9.34 ppm) > (OEP)Os(Et)<sub>2</sub> (9.23 ppm) > (OEP)Os(<sup>*t*</sup>Bu)<sub>2</sub> (9.03 ppm) emphasizes this point. Not surprisingly, therefore, the  $\delta_{\text{meso}}$  peaks of the (OEP)Os(NO)R complexes lie downfield from those of the corresponding (OEP)Os(R)<sub>2</sub> complexes, since the  $\pi$ -acid nitrosyl ligand is an effective withdrawer of electron density from the Os center. Interestingly, the proton resonances for the axial  $\alpha$ -H's in the (OEP)Os(NO)R complexes are shifted significantly upfield from those in the non-nitrosyl (OEP)Os(R)<sub>2</sub> complexes. For example, the axial  $\alpha$ -H resonance for (OEP)Os(NO)Me is at -8.10 ppm while that for (OEP)Os(Me)<sub>2</sub> is at -1.16 ppm. The same trend is observed for the axial  $\alpha$ -H resonance of (OEP)Os(NO)-Et at -7.45 ppm (CH<sub>2</sub>Me), compared with that of (OEP)Os(Et)<sub>2</sub> at -0.72 ppm (CH<sub>2</sub>Me). We are cautious not to over-interpret these trends, however, since many more factors need to be taken into consideration when dealing with the rather complicated metalloporphyrin macrocycle and associated cis- and trans-influences.<sup>62</sup>

(61) Feltham, R. D.; Enemark, J. H. *Top. Stereochem.* **1981**, *12*, 155–215.

(62) Buchler, J. W.; Kokisch, W.; Smith, P. D. *Struct. Bonding* **1978**, *34*, 79–134.

**Nitrosyl Halide Complexes.** As shown in Scheme 1, the (OEP)Os(NO)Cl and (OEP)Os(NO)Br complexes are also formed from the low-temperature reactions of [(OEP)Os(NO)]PF<sub>6</sub> with RMgCl and RMgBr, respectively. In some cases (e.g., the reaction with MeMgBr at low temperature), they are the major isolated products. At room temperature, however, the (OEP)Os(NO)X complexes may also react with RMgX to form (OEP)Os(NO)R. For example, the reaction of (OEP)Os(NO)Br with excess (*p*-C<sub>6</sub>H<sub>4</sub>F)MgBr in THF for 0.5 h gives a 1:1 mixture of (OEP)Os(NO)(*p*-C<sub>6</sub>H<sub>4</sub>F) and (OEP)Os(*p*-C<sub>6</sub>H<sub>4</sub>F)<sub>2</sub>. To the best of our knowledge, these nitrosyl halide compounds have not been reported previously in the literature, although the (OEP)Os(NO)F complex has been known for over 20 years.<sup>63,64</sup> Interestingly, this latter fluoride compound is obtained in 14% yield if (OEP)Os(CO) is reacted with a 2-fold excess of NOPF<sub>6</sub> under laboratory lighting. A higher yield of (OEP)Os(NO)F (92%) is obtained from the reaction of (OEP)Os(NO)Cl with excess AgBF<sub>4</sub> in toluene for 0.5 h. In any event, these (OEP)Os(NO)X (X = F, Cl, Br) compounds are air-stable, showing no signs of decomposition in the solid-state or in solution in air overnight.

As expected, the  $\nu_{\text{NO}}$  of these (OEP)Os(NO)X complexes (1799–1795 cm<sup>-1</sup>) are higher than those of the (OEP)Os(NO)R complexes mentioned in the earlier section. Furthermore, the  $\delta_{\text{meso}}$  peaks in the <sup>1</sup>H NMR spectra of the (OEP)Os(NO)X complexes (10.40–10.41 ppm) are shifted downfield from those of the (OEP)Os(NO)R complexes (10.21–10.23 ppm).

**Nitrosyl Oxo Dimer.** We were intrigued with our observation of a fourth isolable product from the reaction described in Scheme 1. The IR spectrum of this complex revealed a band at 1770 cm<sup>-1</sup> in CH<sub>2</sub>Cl<sub>2</sub> attributable to  $\nu_{\text{NO}}$ . This  $\nu_{\text{NO}}$  is lower than that of the (OEP)Os(NO)X halide complexes just described but is much higher than those of the (OEP)Os(NO)R complexes. However, it is slightly higher than those of (OEP)Os(NO)(*O*-*n*-Bu) (1757 cm<sup>-1</sup>) and (OEP)Os(NO)(*O*-*i*-C<sub>5</sub>H<sub>11</sub>) (1756 cm<sup>-1</sup>) but lower than that of (OEP)Os(NO)(O<sub>2</sub>PF<sub>2</sub>) (1820 cm<sup>-1</sup>),<sup>60</sup> all of which contain axial *O*-bound ligands trans to NO. However, the <sup>1</sup>H NMR spectrum of this complex only showed resonances due to the OEP macrocycle. The  $\delta_{\text{meso}}$  peak is at 10.35 ppm, which is between those of the (OEP)Os(NO)X complexes (10.40–10.41 ppm) and the (OEP)Os(NO)R compounds (10.21–10.24 ppm). Interestingly, this fourth product (Scheme 1) is also obtained as a byproduct in 48% yield from our attempts to generate (OEP)Os(NO)Cl (obtained in 49% yield) from the reaction of (OEP)Os(CO) with ClNO in CH<sub>2</sub>Cl<sub>2</sub>. We were able to obtain a suitable crystal of this complex as an HCl solvate by slow evaporation of a CH<sub>2</sub>Cl<sub>2</sub> solution of the crude product (the source of HCl is probably the ClNO reagent, since concentrated HCl was used in its preparation). The identity of this [(OEP)Os(NO)]<sub>2</sub>( $\mu$ -O) complex was established by a single-crystal X-ray crystallographic analysis of a suitable crystal obtained from the latter reaction.

The molecular structure of [(OEP)Os(NO)]<sub>2</sub>( $\mu$ -O) is shown in Figure 2, and selected bond lengths and angles

**Table 2. Selected Bond Lengths and Angles for [(OEP)Os(NO)]<sub>2</sub>( $\mu$ -O)·2HCl**

Bond Lengths (Å)			
Os(1)–N(1)	2.066(5)	Os(1)–O(2)	2.0945(5)
Os(1)–N(2)	1.778(11)	N(2)–O(1)	1.143(13)
Bond Angles (deg)			
Os(1)–N(2)–O(1)	180.0	N(1)–Os(1)–N(2)	94.2(2)
Os(1)–O(2)–Os(2)	180.0	N(2)–Os(1)–O(2)	180.0
N(1)–Os(1)–O(2)	85.8(2)		

are given in Table 2. To the best of our knowledge, this is the first reported example of a nitrosyl porphyrin  $\mu$ -oxo dimer of any metal (Table 3). The Os–N(porphyrin) bond length of 2.066(5) Å is within the 1.986(9)–2.109(8) Å range observed for other (OEP)Os<sup>II</sup> porphyrins.<sup>65</sup> The Os–N(2) and N(2)–O(1) bond lengths of 1.778(11) and 1.143(13) Å are typical for osmium nitrosyls.<sup>65</sup> The Os–N–O moiety is linear. The Os–( $\mu$ -oxo)–Os group is also linear, with an Os–O(2) bond length of 2.0945(5) Å.

The porphyrin core is domed, and the Os atom is displaced 0.23 Å from the 24-atom mean plane toward the axial NO ligand (Figure 3a). This observed Os displacement is indeed remarkable, since a common feature of porphyrin  $\mu$ -oxo dimers is the displacement of the metal toward the  $\mu$ -oxo bridge.<sup>80</sup> For example, the Os atom is found to be displaced 0.07 Å from the 24-atom porphyrin core toward the  $\mu$ -oxo ligand in the only other structurally characterized osmium porphyrin  $\mu$ -oxo complex, namely [(OEP)Os(OCH<sub>3</sub>)<sub>2</sub>( $\mu$ -oxo)].<sup>79,80</sup> The two porphyrin rings in [(OEP)Os(NO)]<sub>2</sub>( $\mu$ -O) display a twist angle of 22.5° with respect to each other (Figure 3b).

The crystal also contains HCl as a solvate.<sup>57</sup> The close proximity of the HCl molecule to the 4-fold symmetry axis generates a set of four molecules with Cl...Cl distances of 2.02 and 2.85 Å (Figure 4a). The Cl...Cl distance of 2.02 Å is too short to be real and can be explained by the partial occupancy of these sites. The

(65) See Tables 2 and 3 in ref 60 for a listing of structurally characterized osmium nitrosyls and porphyrins.

(66) Chen, B.; Hobbs, J. D.; Debrunner, P. G.; Erlebacher, J.; Shelnett, J. A.; Scheidt, W. R. *Inorg. Chem.* **1995**, *34*, 102–110.

(67) Swepston, P. N.; Ibers, J. A. *Acta Crystallogr.* **1985**, *C41*, 671–673.

(68) Jiao, X.-D.; Huang, J.-W.; Ji, L.-N.; Luo, B.-S.; Chen, L.-R. *J. Inorg. Biochem.* **1997**, *65*, 229–233.

(69) Schaefer, W. P.; Ellis, P. E.; Lyons, J. E.; Shaikh, S. N. *Acta Crystallogr.* **1995**, *C51*, 2252–2255.

(70) Gold, A.; Jayaraj, K.; Doppelt, P.; Fischer, J.; Weiss, R. *Inorg. Chim. Acta* **1988**, *150*, 177–181.

(71) Lay, K.-L.; Buchler, J. W.; Kenny, J. E.; Scheidt, W. R. *Inorg. Chim. Acta* **1986**, *123*, 91–97.

(72) Strauss, S. H.; Pawlik, M. J.; Skowrya, J.; Kennedy, J. R.; Anderson, O. P.; Spartalian, K.; Dye, J. L. *Inorg. Chem.* **1987**, *26*, 724–730.

(73) Karlin, K. D.; Nanthakumar, A.; Fox, S.; Murthy, N. N.; Ravi, N.; Huynh, B. H.; Orosz, R. D.; Day, E. P. *J. Am. Chem. Soc.* **1994**, *116*, 4753–4763.

(74) Landrum, J. T.; Grimmett, D.; Haller, K. J.; Scheidt, W. R.; Reed, C. A. *J. Am. Chem. Soc.* **1981**, *103*, 2640–2650.

(75) Ivanca, M. A.; Lappin, A. G.; Scheidt, W. R. *Inorg. Chem.* **1991**, *30*, 711–718.

(76) Masuda, H.; Taga, T.; Osaki, K.; Sugimoto, H.; Mori, M.; Ogoshi, H. *J. Am. Chem. Soc.* **1981**, *103*, 2199–2203.

(77) Masuda, H.; Taga, T.; Osaki, K.; Sugimoto, H.; Mori, M.; Ogoshi, H. *Bull. Chem. Soc. Jpn.* **1982**, *55*, 3887–3890.

(78) Collman, J. P.; Barnes, C. E.; Brothers, P. J.; Collins, T. J.; Ozawa, T.; Galluci, J. C.; Ibers, J. A. *J. Am. Chem. Soc.* **1984**, *106*, 5151–5163.

(79) Masuda, H.; Taga, T.; Osaki, K.; Sugimoto, H.; Mori, M. *Bull. Chem. Soc. Jpn.* **1984**, *57*, 2345–2351.

(80) See Table 6 in ref 66 for an extensive and informative listing of structural parameters for porphyrin  $\mu$ -oxo dimers.

(63) Buchler, J.; Smith, P. D. *Chem. Ber.* **1976**, *109*, 1465–1476.

(64) Antipas, A.; Buchler, J. W.; Gouterman, M.; Smith, P. D. *J. Am. Chem. Soc.* **1980**, *102*, 198–207.

**Table 3.** Selected Structural Parameters for Group 8 Oxo-Bridged Porphyrin Dimers

compound	M-( $\mu$ -O), Å	M-O-M (deg)	ref
Iron			
[(OEP)Fe] <sub>2</sub> ( $\mu$ -O) triclinic	1.758(3)	172.2(2)	66
	1.754(3)		
monoclinic	1.748(4)	176.21(23)	
	1.762(4)		
[(TPP)Fe] <sub>2</sub> ( $\mu$ -O)	1.759(1)	176.1	67
[(T( <i>p</i> -Cl)PP)Fe] <sub>2</sub> ( $\mu$ -O)	1.743(3)	180.0	68
[(OEP(NO <sub>2</sub> ) <sub>2</sub> )Fe] <sub>2</sub> ( $\mu$ -O)	1.763(4)	167.9(3)	69
	1.751(4)		
[(T(F <sub>5</sub> )PP)Fe] <sub>2</sub> ( $\mu$ -O)	1.775(1)	178.4(5)	70
[(Me <sub>2</sub> OEP)Fe] <sub>2</sub> ( $\mu$ -O)	1.752(1)	178.5(6)	71
[(TPC)Fe] <sub>2</sub> ( $\mu$ -O) <sup>a</sup>	1.747(5)	180.0	72
	1.763(5)		
[(T( <i>o</i> -F <sub>2</sub> )PP)Fe] <sub>2</sub> ( $\mu$ -O)	1.760(2)	178.5(8)	73
[(FF)Fe] <sub>2</sub> ( $\mu$ -O) <sup>b</sup>	1.800(6)	161.1(4)	74
	1.774(6)		
[(TMPyP)Fe] <sub>2</sub> ( $\mu$ -O)·(ClO <sub>4</sub> ) <sub>8</sub>	1.750(2)	175.1(7)	75
[( <i>N</i> -CH <sub>3</sub> TPP)Fe-O-Fe(TPP)]ClO <sub>4</sub>	1.740(4)	165.4(3)	20
	1.767(4) (TPP)		
Ruthenium			
[(OEP)Ru(OH)] <sub>2</sub> ( $\mu$ -O)	1.847(13)	180.0	76
[(OEP)Ru(Cl)] <sub>2</sub> ( $\mu$ -O)	1.793(2)	180.0	77
[(TPP)Ru( <i>p</i> -OC <sub>6</sub> H <sub>4</sub> Me)] <sub>2</sub> ( $\mu$ -O)	1.787(11)	177.8(7)	78
	1.791(11)		
Osmium			
[(OEP)Os(OCH <sub>3</sub> )] <sub>2</sub> ( $\mu$ -O)	1.807(3)	177.4(17)	79
	[1.809(3)] <sup>c</sup>	[179.5(11)] <sup>c</sup>	
[(OEP)Os(NO)] <sub>2</sub> ( $\mu$ -O)	2.0945(5)	180.0	this work

<sup>a</sup> TPC = tetraphenylchlorinato dianion. <sup>b</sup> FF = face-to-face porphyrin. *N,N*-Bis(5-*o*-phenyl)-10,15,20-triphenylporphyrin urea. <sup>c</sup> Two independent dimers. The values for the second dimer are in brackets.

Cl...Cl distance of 2.85 Å is reasonable for a Cl-H...Cl hydrogen bond. A reasonable model for the four HCl molecules is actually two pairs of hydrogen-bonded molecules as shown in Figure 4b. The distances and angles for this hydrogen bond are Cl1-H1 (1.06(5) Å), Cl1...H1<sup>#</sup> (1.95(5) Å), Cl1...Cl1<sup>#</sup> (2.854(5) Å), and Cl1-H1...Cl1<sup>#</sup> (140(3)°) (where # indicates a symmetry equivalent position (-0.5 - *x*, -0.5 - *y*, *z*). These distances are consistent with the reported values for other HCl solid-state structures.<sup>81-86</sup> Partial occupancy of the HCl molecule is not unusual.<sup>87</sup>

**Thionitrosyl Compounds.** To the best of our knowledge, no osmium porphyrin complex containing the NS ligand has been reported, although the related (TTP)Ru(NS)Cl compound is known<sup>88</sup> and the (TPP)-Fe(NS) compound claimed.<sup>53</sup>

The (OEP)Os(NS)Cl compound is prepared in 49% isolated yield from the reaction of (NSCl)<sub>3</sub> with (OEP)-Os(CO) in THF. The IR spectrum of this compound (as a KBr pellet) reveals a band at 1270 cm<sup>-1</sup> assigned to  $\nu_{NS}$ . This value is within the 1065-1390 cm<sup>-1</sup> range observed for other thionitrosyl compounds with linear metal-NS linkages.<sup>89</sup> Furthermore, the use of (<sup>15</sup>-NSCl)<sub>3</sub> in the preparation gives the analogous (OEP)-Os(<sup>15</sup>NS)Cl with a  $\nu_{NS}$  of 1231 cm<sup>-1</sup> ( $\Delta\nu_{NS}$  = 39 cm<sup>-1</sup>),

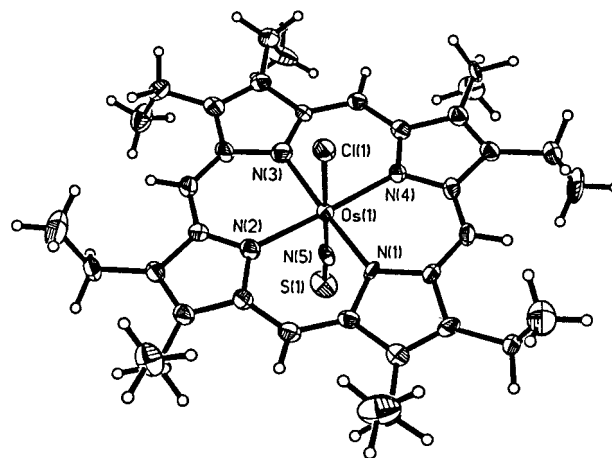


**Figure 5.** Molecular structure of (OEP)Os(NS)Cl. Only the highest occupancy axial Cl-Os-NS orientation is shown.

confirming this assignment of  $\nu_{NS}$ . The  $\delta_{meso}$  in the <sup>1</sup>H NMR spectrum of (OEP)Os(NS)Cl is at 10.49 ppm, which is downfield from that of the nitrosyl (OEP)Os(NO)Cl analogue at 10.41 ppm.

We were able to obtain a suitable crystal for an X-ray diffraction study. The molecular structure is shown in Figure 5, and selected bond lengths and angles are given in Table 4. The Os-N(porphyrin) bond length is 2.065 Å (average) and also falls within the range observed for other structurally characterized (OEP)Os<sup>II</sup> porphyrins.<sup>60,65</sup> The NS and Cl fragments are disordered. The Os-N(S) and (Os)N-S bond lengths are 1.83(1) and 1.50(1) Å, respectively, and are comparable to those of other Os-NS complexes that have been structurally characterized (Table 5). The linearity of the Os-N-S linkage is indicated by an Os-N-S bond angle of 174°. The geometry of the Os-NS moiety is thus reasonable

(81) Mootz, D.; Deeg, A. *J. Am. Chem. Soc.* **1992**, *114*, 5887-5888.

(82) Moynihan, K. J.; Boorman, P. M.; Ball, J. M.; Patel, V. D.; Kerr, K. A. *Acta Crystallogr.* **1982**, *B38*, 2258-2261.

(83) Stepien, A. *Acta Crystallogr.* **1977**, *B33*, 2854-2857.

(84) Mootz, D.; Hocken, J. *Angew. Chem., Int. Ed. Engl.* **1989**, *28*, 1697-1698.

(85) Mootz, D.; Deeg, A. *Z. Anorg. Allg. Chem.* **1992**, *615*, 109-113.

(86) Deeg, A.; Mootz, D. *Z. Naturforsch.* **1993**, *48B*, 571-576.

(87) Boorman, P. M.; Moynihan, K. J.; Richardson, J. F. *Inorg. Chem.* **1988**, *27*, 3207-3211.

(88) Bohle, D. S.; Hung, C.-H.; Powell, A. K.; Smith, B. D.; Wocadlo, S. *Inorg. Chem.* **1997**, *36*, 1992-1993.

(89) Chivers, T.; Edelmann, F. *Polyhedron* **1986**, *5*, 1661-1699.

**Table 4. Selected Bond Lengths and Angles for (OEP)Os(NS)Cl<sup>a</sup>**

Bond Lengths (Å)			
Os(1)–N(5)	1.832(13) [1.834(13)]	Os(1)–N(2)	2.072(6)
N(5)–S(1)	1.501(12) [1.502(12)]	Os(1)–N(3)	2.075(9)
Os(1)–Cl(1)	2.329(3) [2.327(4)]	Os(1)–N(4)	2.063(5)
Os(1)–N(1)	2.050(7)		
Bond Angles (deg)			
Os(1)–N(5)–S(1)	174.5(14) [174(2)]	N(2)–Os(1)–Cl(1)	90.0(2) [90.4(8)]
Cl(1)–Os(1)–N(5)	177.7(7) [176.4(10)]	N(2)–Os(1)–N(3)	90.2(3)
N(1)–Os(1)–N(5)	92.1(6) [84.2(12)]	N(2)–Os(1)–N(4)	176.4(2)
N(1)–Os(1)–Cl(1)	89.7(3) [92.4(7)]	N(3)–Os(1)–N(5)	91.6(7) [92.1(11)]
N(1)–Os(1)–N(2)	90.2(3)	N(3)–Os(1)–Cl(1)	86.7(2) [91.2(7)]
N(1)–Os(1)–N(3)	176.3(4)	N(3)–Os(1)–N(4)	89.6(3)
N(1)–Os(1)–N(4)	89.8(2)	N(4)–Os(1)–N(5)	92.1(7) [88(2)]
N(2)–Os(1)–N(5)	91.6(7) [88(2)]	N(4)–Os(1)–Cl(1)	86.4(2) [93.3(8)]

<sup>a</sup> Numbers in square brackets are for the minor (19%) disordered Cl(1')–Os(1)–N(5')–S(1') component.

**Table 5. Selected Structural Data for Group 8 Thionitrosyl Complexes<sup>a</sup>**

compound	M–N (Å)	N–S (Å)	M–N–S (deg)	ref
Osmium				
Os(NS)Cl <sub>3</sub> (PPh <sub>3</sub> ) <sub>2</sub>	1.779(9)	1.503(10)	180.0(1)	90
(PPh <sub>4</sub> ) <sub>2</sub> [Os(NS)Cl <sub>4</sub> (H <sub>2</sub> O)]	1.731(4)	1.514(5)	174.9(3)	91
(AsPh <sub>4</sub> ) <sub>2</sub> [Os(NS)(NSCl)Cl <sub>4</sub> ] <sup>b</sup>	1.828(8)	1.46(1)	169.1(5)	92
(OEP)Os(NS)Cl <sup>c</sup>	1.832(13)	1.501(12)	174.5(14)	this work
Ruthenium				
(PPh <sub>4</sub> ) <sub>2</sub> [Ru(NS)Cl <sub>4</sub> (H <sub>2</sub> O)]	1.729(4)	1.504(4)	170.9(3)	93
(PPh <sub>4</sub> ) <sub>2</sub> [Ru(NS)Cl <sub>4</sub> ] <sub>2</sub> ·4CH <sub>2</sub> Cl <sub>2</sub>	1.752(6)	1.466(7)	177.3(5)	94
(PPh <sub>4</sub> ) <sub>2</sub> {[Ru(NS)Br <sub>4</sub> ] <sub>2</sub> (μ-N <sub>2</sub> S <sub>2</sub> )}·4CH <sub>2</sub> X <sub>2</sub> <sup>d</sup>	1.69(3)	1.51(3)	175(2)	95
(TTP)Ru(NS)Cl <sup>e</sup>	1.768(4)	1.489(5)	169.1(3)	88
	[1.85(3)]	[1.47(3)]	[170(3)]	

<sup>a</sup> The data for (OEP)Os(NS)Me (this work) are not included because of the nature of the disorder, which precludes comparisons with other M–NS complexes. <sup>b</sup> The Cl atom of NSCl is disordered over the NS and NSCl ligands. <sup>c</sup> Data are for the 81% occupancy component. <sup>d</sup> Contains CH<sub>2</sub>Cl<sub>2</sub> and CH<sub>2</sub>Br<sub>2</sub> molecules (i.e., X = Cl, Br). <sup>e</sup> Two independent molecules. Data for the second (disordered) molecule are given in brackets and were obtained from the Supporting Information via the Internet.

(Table 5). Importantly, the M–N(S) bond lengths for other (nongroup 8) metal thionitrosyl complexes range from 1.694(2) (M = Cr)<sup>96</sup> to 1.87(2) Å (M = Re).<sup>97</sup> MN–S bond lengths for these nongroup 8 compounds range from 1.38(2) (M = Re)<sup>98</sup> to 1.592(11) Å (M = Mo),<sup>99</sup> whereas M–N–S bond angles range from 170.0(4)° (M = Tc)<sup>100</sup> to 179.9(1)° (M = Tc).<sup>101</sup>

The spectroscopically pure (OEP)Os(NS)Me compound is generated in 23% yield from the reaction of (OEP)Os(NS)Cl with MeMgBr in THF. We have not been able to obtain sizable amounts of a pure sample of this compound for a satisfactory combustion analysis. This compound is light and air sensitive and is also very difficult to separate from the (OEP)Os(Me)<sub>2</sub> byproduct

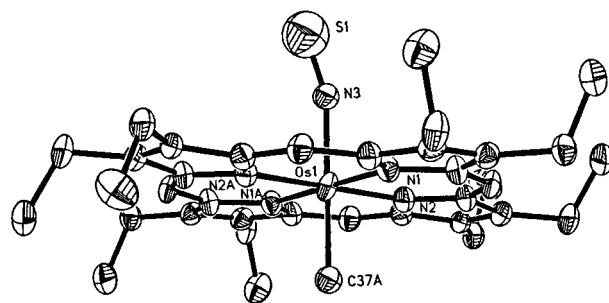


**Figure 6.** Molecular structure of (OEP)Os(NS)Me. Only one of the two disordered axial SN–Os–Me orientations is shown.

(also obtained in 14% yield). In any event, the  $\nu_{\text{NS}}$  of (OEP)Os(NS)Me is at 1196 cm<sup>-1</sup> ( $\nu_{15\text{NS}} = 1163$  cm<sup>-1</sup>), reflecting the electron-donating nature of the axial methyl group compared with the precursor chloride. The  $\delta_{\text{meso}}$  in the <sup>1</sup>H NMR spectrum of the (OEP)Os(NS)Me compound is at 10.30 ppm, which is shifted upfield by 0.19 ppm from that of the chloro (OEP)Os(NS)Cl precursor (at 10.49 ppm) but is shifted *downfield* from that of its nitrosyl (OEP)Os(NO)Me analogue (at 10.21 ppm). Interestingly, the  $\delta_{\text{meso}}$  peak of (OEP)Os(NO)Me is also shifted (by 0.20 ppm) upfield from that of its chloro precursor. Attempts to generate other (OEP)Os(NS)R compounds have not yet been successful, and other routes are being sought for their syntheses.

The molecular structure of (OEP)Os(NS)Me is shown in Figure 6, and selected bond lengths and angles are given in Table 6. The most important feature is the confirmation of the identities of the trans methyl and thionitrosyl ligands. The Os–N(porphyrin) bond lengths

(90) Roesky, H. W.; Pandey, K. K.; Clegg, W.; Noltemeyer, M.; Sheldrick, G. M. *J. Chem. Soc., Dalton Trans.* **1984**, 719–721.

(91) Pandey, K. K.; Roesky, H. W.; Noltemeyer, M.; Sheldrick, G. M. *Z. Naturforsch.* **1984**, *39b*, 590–593.

(92) Weber, R.; Müller, U.; Dehnicke, K. *Z. Anorg. Allg. Chem.* **1983**, *504*, 13–22.

(93) Bats, J. W.; Pandey, K. K.; Roesky, H. W. *J. Chem. Soc., Dalton Trans.* **1984**, 2081–2083.

(94) Willing, W.; Müller, U.; Demant, U.; Dehnicke, K. *Z. Naturforsch.* **1986**, *41b*, 560–566.

(95) Demant, U.; Willing, W.; Müller, U.; Dehnicke, K. *Z. Anorg. Allg. Chem.* **1986**, *532*, 175–183.

(96) Greenhough, T. J.; Kolthammer, B. W. S.; Legzdins, P.; Trotter, J. *Inorg. Chem.* **1979**, *18*, 3548–3554.

(97) Ruf, C.; Behrens, U.; Lork, E.; Mews, R. *Chem. Commun.* **1996**, 939–940.

(98) Hauck, H.-G.; Willing, W.; Müller, U.; Dehnicke, K. *Z. Naturforsch.* **1986**, *41b*, 825–830.

(99) Hursthouse, M. B.; Motevalli, M. *J. Chem. Soc., Dalton Trans.* **1979**, 1362–1366.

(100) Lu, J.; Clarke, M. J. *J. Chem. Soc., Dalton Trans.* **1992**, 1243–1248.

(101) Kaden, L.; Lorenz, B.; Kirmse, R.; Stach, J.; Behm, H.; Beurskens, P. T.; Abram, U. *Inorg. Chim. Acta* **1990**, *169*, 43–48.

**Table 6. Selected Bond Lengths and Angles for (OEP)Os(NS)Me<sup>a</sup>**

Bond Lengths (Å)			
Os(1)–N(3)	1.999(8)	Os(1)–N(1)	2.056(7)
N(3)–S(1)	1.433(13)	Os(1)–N(2)	2.055(7)
Os(1)–C(37A)	1.999(8)		
Bond Angles (deg)			
Os(1)–N(3)–S(1)	163.0(8)	N(1)–Os(1)–N(2)	90.4(3)
C(37A)–Os(1)–N(3)	180.0	N(2)–Os(1)–C(37A)	89.6(3)
N(1)–Os(1)–N(3)	91.5(3)	N(2)–Os(1)–N(3)	90.4(3)
N(1)–Os(1)–C(37A)	88.5(3)		

<sup>a</sup> The axial methyl (C37A or C37) and NS (N3 and S1) groups are completely disordered, and attempts to refine C37 and N3 with slightly different positional parameters yielded poor and unstable refinement. The C37 and N3 atoms were assigned identical positional and thermal parameters, which gave more stable refinement.

are 2.056(7) and 2.055(7) Å. Unfortunately, the nature of the axial disorder (see Experimental Section) precludes a comparison of the bond lengths and angles involving these axial groups.

In summary, we have reported the synthesis and characterization of a new series of (i) organoosmium nitrosyl and thionitrosyl porphyrins, (ii) osmium nitrosyl and thionitrosyl halide porphyrins, and (iii) organoos-

mium bis-alkyl/aryl porphyrins. We have also reported the synthesis and structural characterization of a novel osmium nitrosyl  $\mu$ -oxo dimer. Studies are currently underway to exploit the nature and reactivity of the metal–carbon bond in these and related complexes.

**Acknowledgment.** We are grateful to the National Institutes of Health (FIRST Award 1R29 GM53586-01A1) and the National Science Foundation (CAREER Award CHE-9625065) for funding of this research. We thank Dr. J. W. Buchler (Germany) for helpful discussions. We also thank S. J. Hodge for initial experiments involving related (TTP)Os(NO)- and (TTP)Os(NS)-containing systems.<sup>102</sup>

**Supporting Information Available:** Figures and tables of crystal data, atomic coordinates, anisotropic displacement parameters, bond lengths and angles, hydrogen coordinates and isotropic displacement parameters, torsion angles, and least-squares planes (40 pages). Ordering information is given on any current masthead page.

OM980197S

(102) Hodge, S. J. Ph.D. Dissertation, University of Oklahoma, 1998.